

The Machine Learning Control Method for Counterfactual Forecasting*

Augusto Cerqua

Department of Social Sciences and Economics, Sapienza University of Rome
email: augusto.cerqua@uniroma1.it

Marco Letta

Department of Social Sciences and Economics, Sapienza University of Rome
email: marco.letta@uniroma1.it

Fiammetta Menchetti

Department of Statistics, Computer Science and Applications, University of Florence
email: fiammetta.menchetti@unifi.it

December 12, 2023

Abstract

Without a credible control group, the most widespread methodologies for estimating causal effects cannot be applied. To fill this gap, we propose the Machine Learning Control Method (MLCM), a new approach for causal panel analysis based on counterfactual forecasting with machine learning. The MLCM estimates policy-relevant causal parameters in short- and long-panel settings without relying on untreated units. We formalize identification in the potential outcomes framework and then provide estimation based on supervised machine learning algorithms. To illustrate the advantages of our estimator, we present simulation evidence and an empirical application on the impact of the COVID-19 crisis on educational inequality in Italy. We implement the proposed method in the companion R package `MachineControl`.

Keywords: potential outcomes framework, counterfactual forecasting, machine learning, short panel, panel cross-validation, education inequality

JEL-Codes: C13, C18, C53, I24

We are grateful to Guido Imbens and Fabrizia Mealli for thoughtful conversations and discussions. We also thank Andrea Albanese, Guglielmo Barone, Michele Battisti, Alessio D’Ignazio, Christina Gatmann, Anna Gottard, Giulio Grossi, Martin Huber, Michael Knaus, Joanna Kopinska, Giuseppe Maggio, Alessandra Mattei, Raffaele Mattera, Giovanni Mellace, Andrea Mercatanti, Samuel Nocito, Jason Poulos, Donato Romano, Jacques-François Thisse, Luca Tiberti, Giuseppe Ragusa and Giuliano Resce for valuable suggestions on earlier versions of this work. The paper has also benefited from many helpful comments and suggestions by audiences at the 2023 LISER International Workshop on “Machine Learning in Program Evaluation, High-dimensionality and Visualization Techniques”, the Oslo 2023 European Causal Inference Meeting, the AISRe, COMPIE, and SIE 2022 annual conferences and seminar participants at the Florence Center for Data Science and Sapienza University of Rome. We thank Gabriele Pinto and Federico Rucci for useful comments on the implementation.

“In history there are no control groups. There is no one to tell us what might have been.”
Cormac McCarthy, *All the Pretty Horses* (1992)

1 Introduction

Today, the econometric toolbox for causal panel analysis features many alternative approaches for estimating causal effects, such as difference-in-differences (Card and Krueger, 1994), the synthetic control method (Abadie et al., 2010), two-way (Angrist and Pischke, 2009) and interactive (Bai, 2009) fixed effects models, and matrix completion methods (Athey et al., 2021). However, all of these popular methodologies depend on a critical requirement: the availability of untreated units forming a credible control group, without which they cannot be applied. This poses a relevant econometric challenge in observational studies, as there are at least two relevant cases in which a control group does not exist: (i) the treatment simultaneously affects all units, as in the case of a large-scale shock or a nationwide program with universal participation (Duflo, 2017)¹; (ii) only a subgroup of units gets treated, but the set of untreated units cannot form a valid control group due to violations of the no-interference assumption (Cox, 1958).² Under these challenging but not uncommon circumstances, the use of standard causal panel data methods is precluded, leaving a gap in the econometric toolkit of empirical researchers.

We fill this gap by introducing the Machine Learning Control Method (MLCM), a new estimator based on flexible counterfactual forecasting via machine learning (ML). The MLCM is a versatile technique that can leverage any available supervised ML algorithm and enables the estimation of several policy-relevant causal parameters—including individual, average, and conditional average treatment effects (CATEs)—in evaluation settings with short and long panels and no control group. The intuition behind the MLCM is straightforward: when you cannot rely on untreated units to build the counterfactual, you can forecast it. Specifically, use supervised ML techniques trained and tuned on the pre-treatment data to forecast the evolution of post-treatment outcomes in the absence of the treatment. Then, estimate treatment effects as the difference between observed and forecasted post-treatment outcomes.

Our approach builds upon and bridges three different methodological currents: causal panel data methods, time series forecasting, and causal ML. From the literature on causal panel analysis, we take the conceptual and identification framework based on the potential outcomes model (Rubin, 1974). Since earlier contributions (Ashenfelter and Card, 1985; Card, 1990) to its more recent developments (Arkhangelsky et al., 2021; Roth et al., 2023), this whole literature ultimately revolves around solving the “fundamental problem of causal inference” (Holland, 1986) in an observational panel data setting. To this end, all existing methodologies leverage untreated units to estimate the counterfactual scenario, i.e., how the outcome of the treated group would have evolved in the absence of the treatment. After building a credible control group, the causal effect is recovered as the difference in outcomes between the two groups. Central to our work is also the perspective of causal inference as a missing data problem, where the key goal is the imputation of missing potential outcomes (Imbens and Rubin,

¹This case also encompasses situations where the treatment simultaneously affects most units, and the remaining ones are too few and too different to constitute a valid control group (even if using synthetic control methods).

²Spillovers are common in many economic settings where the observations are correlated in time, space, or both, and ignoring them can lead to very misleading inferences (Sobel, 2006). In principle, spillovers can be modeled and accounted for at the cost of additional and often restrictive assumptions. However, in practice, most methods just postulate the absence of interference.

2015). We contribute to this literature by introducing a novel estimator that imputes missing potential outcomes and, in turn, gauges causal effects without relying on untreated units.

The time series literature features some forecasting approaches that researchers have employed for counterfactual building in scenarios without a control group. Some of them are straightforward: the mean method estimates the counterfactual “no-treatment scenario” of the dependent variable Y_i as the average of its pre-treatment values, while the naive method considers the last pre-treatment value of Y_i as the counterfactual (Hyndman and Athanasopoulos, 2021). A more sophisticated forecasting approach is the interrupted time series (ITS) analysis, first formalized by Box and Tiao (1975). ITS analysis generally fits regression models or autoregressive integrated moving average (ARIMA) models to the entire time series of observed data; this is done after postulating a structure on the intervention effect (e.g., constant level shift). By construction, ITS delivers a single average effect for the whole post-intervention period. More recent studies (Brodersen et al. (2015), Chernozhukov et al. (2021), Menchetti et al. (2023)) have formalized estimation and inference with time series forecasting techniques (such as ARIMA) within the potential outcomes framework. However, such methods are designed for cases with a single treated series, often impose restrictive functional forms, and can be implemented only when at least tens of pre-treatment periods are available.³ We draw from this literature the idea of forecasting the counterfactual when no control group is available and the estimation approach based on temporal cross-validation. We add to it by proposing a flexible, ML-powered forecasting technique suitable for panel data and able to estimate separate effects for multiple post-intervention periods.

In recent years, a new literature at the intersection between causal inference with panel data and ML has evolved. Causal trees and forests (Athey and Imbens (2016), Wager and Athey (2018)) constitute an adaptation of tree-based predictive models to the task of estimating heterogeneous treatment effects, and can be applied to both randomized and observational data. Although they are not specifically designed for panel settings, they can also be employed with panel data (e.g., Athey et al. (2023); Britto et al. (2022)). Artificial control methods (Carvalho et al. (2018), Masini and Medeiros (2021)) and the synthetic learner proposed by Viviano and Bradic (2023) harness supervised ML algorithms to predict counterfactuals and assess treatment effects in a panel setting with a single treated unit, many untreated peers, and a long pre-intervention window. Nevertheless, in order to build a counterfactual scenario, all these causal ML techniques need a set of units assumed to be completely unaffected by the treatment. We borrow from this literature the idea of harnessing the power of ML in the service of causal inference rather than for pure prediction, exploiting the fact that counterfactual building is ultimately a predictive task (Varian, 2016). We extend it by proposing a ML estimator that: i) does not depend on the availability of untreated units or on the no-interference assumption; ii) is designed for situations with many treated units; iii) also works with a few pre-treatment periods.

After discussing identification in the potential outcomes framework, we propose an estimation strategy based on a horse-race competition between several different ML algorithms, panel cross-validation (CV) for model selection, and block-bootstrapping for inference. The MLCM comes with a set of diagnostic, performance, and placebo tests and is characterized by a high level of generality: it delivers individual treatment effects that can either be the object of interest or can later be aggregated into several policy-relevant causal estimands. Since our approach allows for arbitrary and unrestricted treatment effect heterogeneity, we also propose an automated search for heterogeneity based on an

³Closely related to these time series approaches, Botosaru et al. (2023) propose the use of simple techniques, such as polynomial regressions, to estimate treatment effects one period after the implementation of the treatment in panel settings without controls.

easy-to-interpret regression tree. To showcase the potential of the MLCM, we present a simulation study and an empirical application in which we investigate the effects of the COVID-19 pandemic on educational inequality in Italian Local Labor Markets (LLMs). We find that the pandemic led to a generalized drop in students’ performance, which is particularly pronounced in LLMs that before COVID-19 were characterized by higher levels of unemployment and inequality and lower educational attainment.

The possibility of moving beyond the reliance on untreated units paves the way to evaluating many potential treatments—such as universal policies, large-scale shocks, and programs engendering interactions between units—that, due to the lack of a valid comparison group, have so far been underexplored in empirical studies. To answer these causal questions, interested researchers can implement the MLCM on real-world datasets using the companion R package `MachineControl`.⁴

The rest of this paper is organized as follows. Section 2 outlines the causal framework by defining the identification assumptions, the causal estimands, and the estimators. Section 3 describes the implementation process of the MLCM and presents the simulation study. Section 4 illustrates the empirical application. Section 5 concludes.

2 The causal framework

In this section, we present the causal framework for an observational short-panel setup where the intervention is a simultaneous policy change or shock that affects directly or indirectly the entire statistical population under scrutiny.⁵ In such a setting, the estimation of causal effects must rely on estimators specifically designed for scenarios without a control group. We start by defining the causal assumptions and the corresponding causal estimands within the potential outcomes framework. We then provide the proof that such estimands can be identified under those assumptions. Finally, we specify the modeling assumptions and introduce novel estimators for scenarios without untreated units. To make the notation (and the method) as general as possible, the definitions given in this section assume the presence of some contemporaneous covariates unaffected by the intervention. Including these covariates in the MLCM can potentially mitigate certain assumptions. However, as we will discuss later, caution must be exercised in their use and selection.

2.1 Causal assumptions

We need three assumptions to define, identify, and estimate the causal estimands of interest.

Denote with $Y_{i,t}$ the outcome of unit i at time t , and let $W_{i,t} \in \{0, 1\}$ be a random variable describing the treatment assignment of unit $i = 1, \dots, N$ at time $t = 1, \dots, t_0, \dots, T$, where 1 indicates the treatment, 0 indicates control, and t_0 denotes the intervention date.⁶ As we are focusing on a single and simultaneous intervention, we can then write $W_{i,t} = 0$ for all i and $t \leq t_0$, $W_{i,t} = 1$ for all i and $t > t_0$, therefore, $t_0 + 1$ is the first post-intervention period. In other words, the units become treated at the same time and then stay treated. Under the potential outcomes framework, for each unit we can define a potential outcome under $W_{i,t} = 0$ and a different potential outcome under $W_{i,t} = 1$.

The first assumption establishes the crucial link between potential outcomes and treatment assignment. We rely on a less stringent version of the Stable Unit Treatment Value Assumption (SUTVA)

⁴The latest version of the package is available on GitHub at [this link](#).

⁵We take the benchmark case of a balanced panel, but the MLCM accommodates also the use of unbalanced panels.

⁶The word “treatment” is commonly used in the context of randomized controlled trials. As we are dealing with an observational study, we use the terms “treatment”, “intervention”, “policy”, and “shock” interchangeably.

(Rubin, 1974; Imbens and Rubin, 2015). Specifically, we substantially relax SUTVA, retaining only its second part: the treatment is the same for all the units. This is an *a priori* assumption that the potential outcomes do not depend on different treatment intensities or the mechanism used to assign the treatment.

Assumption 1 *There are no hidden forms of treatment leading to different potential outcomes.*

While we maintain this no-multiple-versions-of-treatment assumption, we drop the first part of SUTVA, namely, the no-interference assumption (Cox, 1958).⁷ We consider this as one of the main advantages of our approach because, while it has long been known that violations and failures of the no-interference assumption can lead to misleading inferences in many social science settings (Sobel, 2006), this strong assumption is rarely questioned or tested in practice (Chiu et al., 2023). This is a key departure from most evaluation methods and, therefore, it is important to delve into its implications. SUTVA-related interference among units can be of two types: (1) from treated to control units, and (2) among treated units themselves.⁸ First, we completely circumvent pitfalls regarding Type-1 interference, since our counterfactual scenario is generated without relying on untreated units. Second, we do not postulate the lack of interference among treated units and allow for any possible Type-2 interference. We avoid relying on the no-interference-among-treated assumption because we are aware of the likely presence of interference across both the temporal and cross-sectional dimensions in social science applications (Xu, 2023). Our focus is on estimating the *total* effect of the treatment, rather than on disentangling its direct and indirect effects. The total effect encompasses both the direct effect on a unit from the treatment it receives and the indirect effects arising from the spillover and general equilibrium effects. We claim that in real-world scenarios with likely interaction between units, focusing on the total effect of the treatment is a sensible choice as it captures the actual impact on each unit under the realized treatment assignment mechanism.⁹ Under Assumption 1 we can then write $Y_{i,t}(w_{i,t})$ to indicate the potential outcomes, where the lower case $w_{i,t}$ denotes a realization of $W_{i,t}$.

The next assumption rules out the possibility of anticipatory effects of the intervention on both the outcome and the covariates (Abadie et al., 2010; Borusyak et al., 2023).

Assumption 2 *Let $\mathbf{X}_{i,t} = (X_{i,t}^{(1)}, \dots, X_{i,t}^{(m)})$ be an m -dimensional vector of covariates that are predictive of the outcome i at time $t \leq t_0$; both the covariates and the potential outcomes are unaffected by the policy for all $t \leq t_0$, i.e., $Y_{i,t}(1) = Y_{i,t}(0)$ and $\mathbf{X}_{i,t}(1) = \mathbf{X}_{i,t}(0)$. Some of the covariates are also unaffected by the policy in the post-intervention period, i.e., for all $t > t_0$, $\mathbf{X}_{i,t}(1) = \mathbf{X}_{i,t}(0)$.*

This assumption implies that in the pre-intervention period, the observed outcome corresponds to the potential outcome absent the policy, i.e., $Y_{i,t} = Y_{i,t}(0)$. Additionally, Assumption 2 precludes any anticipatory actions by economic agents, implying that they cannot alter or manipulate their

⁷Following Imbens and Rubin (2015), we consider the case with general equilibrium effects as a scenario in which there are widespread violations of the no-interference assumption. Hence, general equilibrium effects are an example of substantial interaction between units, rather than a separate category.

⁸Even if the treatment is the same for all units, residual spillover effects may arise due to interference among the treated units. Consider, for example, a study investigating excess mortality from COVID-19. While the pandemic affects all areas, those with fewer intensive care beds may need to send patients to neighboring hospitals, prompting an additional (indirect) rise in mortality rates there also. Spillovers due to individuals' characteristics within the same treatment group are discussed in Ogburn and VanderWeele (2014).

⁹In the rare cases in which there will be no Type-2 interference, then the MLCM will retrieve the direct effect of the treatment on each unit, which will coincide with the unit-specific total effect.

outcomes prior to receiving the treatment. This assumption can be empirically tested by verifying whether pre-treatment effects are, on average, zero. Finally, the second part of Assumption 2 (post-treatment exogeneity of the covariates) is only necessary if post-treatment covariate values are used to control for post-treatment confounders (Brodersen et al., 2015). Although motivating covariates' choice is often sufficient, it can be also verified by testing for the presence of treatment effects on each covariate: those that are significantly impacted by the intervention must be removed from the model.

We then make a conditional stationarity assumption (D'Haultfoeuille et al., 2023; Hoderlein and White, 2012).

Assumption 3 *Let \mathcal{I}_0 be the information set up to time $t = 0$, and denote with*

$f_{Y_{i,t+1}(0)|\mathcal{I}_t, \mathbf{X}_{i,t+1}}(y_{i,t+1}(0)|\mathcal{I}_t, \mathbf{X}_{i,t+1})$ the conditional density of the potential outcomes in the absence of the policy, where $\mathcal{I}_t = \{\mathcal{I}_0, \mathbf{X}_{i,1}, \dots, \mathbf{X}_{i,t}, Y_{i,1}(0), \dots, Y_{i,t}(0)\}$. Then,

$$f_{Y_{i,t+1}(0)|\mathcal{I}_t, \mathbf{X}_{i,t+1}}(y_{i,t+1}(0)|\mathcal{I}_t, \mathbf{X}_{i,t+1}) = f_{Y_{i,1}(0)|\mathcal{I}_0, \mathbf{X}_{i,1}}(y_{i,t+1}(0)|\mathcal{I}_t, \mathbf{X}_{i,t+1}).$$

Put simply, the distribution of the potential outcome absent the policy is constant for time translations, conditioned on the information set. Therefore, if we assume to know this distribution in the pre-intervention period, we would also know it in the post-intervention period. This assumption allows forecasting the path of $Y_{i,t}(0)$ in the post-intervention period based on the knowledge gained from the pre-intervention period, and using it as a reliable estimator of the counterfactual potential outcome. While it is not possible to explicitly test for conditional stationarity, we can assess how well the model fits the pre-intervention data via a rigorous panel CV procedure (see Section 3).¹⁰ Assumption 3 implies the absence of other unforecastable shocks or policies affecting the outcome of interest in the post-intervention window. This means that the MLCM attributes any post-intervention divergence from the forecasted counterfactual only to the intervention under scrutiny.

The plausibility of this assumption hinges on institutional and contextual knowledge and requires a careful case-by-case evaluation by the researcher. Compared to popular techniques applied in the canonical setting, such as difference-in-differences and the synthetic control method, this assumption appears stronger, since those techniques can control for common shocks under the assumption that they affect treated and control units in the same way. However, in our framework, the inclusion of contemporaneous covariates plausibly unaffected by the intervention (but correlated with the outcome in the pre-intervention window) plays a similar role in that it helps controlling for changes unrelated to the treatment.¹¹

More generally, the causal framework of the MLCM is characterized by a key trade-off between the plausibility of conditional stationarity (Assumption 3) and the credibility of the exogeneity of the covariate set (Assumption 2). The solution to the trade-off depends on the specific context of each application. For instance, in a study about the impact of a simultaneous but sector-specific policy change on a given outcome of interest, it might be reasonable to assume that other variables remain unaffected by the policy. Examples include a national abortion law, the EU General Data Protection

¹⁰This assumption is closely related to Assumption 2. To see this, let us assume that the intervention produced an effect on the outcome before its implementation: this would inevitably alter the conditional distribution of the potential outcome, and, as a result, Assumption 3 would no longer be valid. Therefore, another way to strengthen the plausibility of this assumption is to check the forecasting performance of the assumed model by shifting the intervention date artificially backward in time.

¹¹To the extent that unit-specific confounders (captured by post-treatment covariates) matter more than common factors (captured by simultaneous controls in the canonical setting) as identification threats, this could make Assumption 3 more credible than the common trends assumption underlying traditional methods. This is especially true since the latter, unlike the former, must be necessarily coupled with the no-interference assumption.

Regulation, the introduction of a restrictive immigration policy, or import bans on products from a sanctioned country. For all these cases, it might be possible to come up with several predictive covariates which will likely be unaffected by the intervention at least in the short-term. In contrast, in contexts where the treatment is a large-scale, simultaneous shock with generalized impacts, such as a recession, a war, or a pandemic (as in our application, see Section 4), assuming post-treatment covariate exogeneity becomes less credible and should be avoided.¹² In all cases, however, it is important to acknowledge that as one moves away from the intervention date, the estimates become less credible. Indeed, not only does Assumption 3 become gradually less plausible, but post-treatment covariates may themselves become contaminated by the treatment, just as can occur with untreated units in the canonical setting (Masini and Medeiros, 2021).

2.2 Causal estimands

In panel settings, the number of possible causal quantities increases substantially. This subsection outlines estimands that could be of general interest for observational studies based on panel data in the absence of control units. We also frame them under a finite-sample perspective, since the MLCM is thought for econometric settings in which the treatment affects, either directly or indirectly, the entire population under study.¹³ The causal estimands discussed here pertain to Case (i) defined above, namely, when the treatment affects all, or most, of the available units, simultaneously. In Appendix C, we also define causal estimands for the Case (ii) scenario with violations of the no-interference assumption. We can first define the Average Treatment Effect (ATE) across units at a given point in time.

Definition 1 *For any strictly positive integer $k = 1, \dots, T - t_0$, let $\tau_{i,t_0+k} = Y_{i,t_0+k}(1) - Y_{i,t_0+k|t_0}(0)$ denote the unit-level effect of the policy at time $t_0 + k$, where $Y_{i,t_0+k|t_0}(0)$ is defined as the expectation of the potential outcome absent the policy given the information set, i.e., $Y_{i,t_0+k|t_0}(0) = E[Y_{i,t_0+k}(0)|\mathcal{I}_{t_0}, \mathbf{X}_{i,t_0+k}]$. Then, the ATE at time $t_0 + k$ is defined as,*

$$\tau_{t_0+k} = \frac{1}{N} \sum_{i=1}^N \tau_{i,t_0+k} = \frac{1}{N} \sum_{i=1}^N Y_{i,t_0+k}(1) - Y_{i,t_0+k|t_0}(0).$$

Note that in this benchmark scenario (Case (i)), the term $t_0 + k$ corresponds to the Average Treatment effect on the Treated (ATT).

The subsequent estimand measures the average effect within a subset of units with the same values of selected covariates. This is commonly referred to as the CATE, and it is of particular interest when there is reason to believe that the intervention has produced heterogeneous effects on different subpopulations of units as defined by their distinct characteristics. Following existing literature on CATE in high-dimensional settings with a mix of discrete and continuous covariates (Fan et al., 2022; Chernozhukov et al., 2018; Knaus et al., 2021), we focus on its low-dimensional summary called “group-average treatment effect”.

¹²Even in these cases, there may be covariates that remain unaffected, such as climate variables. The question is whether these variables are informative or helpful in controlling for potential confounders or structural breaks unrelated to the intervention.

¹³For further details on the difference between the finite-sample and superpopulation perspective in causal inference see Imbens and Rubin (2015). In observational panel settings only Rambachan and Roth (2023) defined causal estimands when the entire population is observed, but their approach still relies on control units.

Definition 2 Let $G_{i,t}$ denote a set of individual characteristics and indicate with N_g the number of units in the population having $G_{i,t} = g$. For any strictly positive integer k , the group CATE at time $t_0 + k$ is defined as,

$$\tau_{t_0+k}(g) = \frac{1}{N_g} \sum_{i:G_{i,t_0+k}=g} \tau_{i,t_0+k}.$$

Note that the set of candidate conditioning variables $G_{i,t}$ used to determine CATEs does not necessarily have to match those utilized for counterfactual forecasting. This is because the variables that predict outcomes can, and often do, differ at least partially from those that predict treatment effect heterogeneity. We also remark that in a general panel setting with more than one post-treatment periods, the above definitions imply the existence of vectors representing estimated average effects, i.e., $\boldsymbol{\tau} = (\tau_{t_0+1}, \dots, \tau_{t_0+k}, \dots, \tau_T)$ and $\boldsymbol{\tau}(g) = (\tau_{t_0+1}(g), \dots, \tau_{t_0+k}(g), \dots, \tau_T(g))$. Furthermore, sometimes researchers are also interested in temporal aggregations of such effects.

Definition 3 The temporal average ATE and CATE are defined, respectively, as,

$$\bar{\tau} = \frac{1}{T - t_0} \sum_{k=1}^{T-t_0} \tau_{t_0+k}$$

$$\bar{\tau}(g) = \frac{1}{T - t_0} \sum_{k=1}^{T-t_0} \tau_{t_0+k}(g).$$

We now prove that under the Assumptions outlined in Section 2.1, the unit-level effect, the ATE and the CATE can be identified from available data.

2.2.1 Identification proof

In Definition 1, $Y_{i,t_0+k}(1)$ is the observed outcome under treatment, which is immediately identified from the data, and $Y_{i,t_0+k|t_0}(0) = E[Y_{i,t_0+k}(0)|\mathcal{I}_{t_0}, \mathbf{X}_{i,t_0+k}]$ is the expected value of the potential outcome absent the treatment conditioning on all the pre-intervention information set, $\mathcal{I}_{t_0} = \{Y_{i,t_0}(0), \dots, Y_{i,1}(0), \mathbf{X}_{i,t_0}, \dots, \mathbf{X}_{i,1}\}$, and contemporaneous covariates. Notice that \mathcal{I}_{t_0} contains the following information: (i) pre-intervention covariates; (ii) pre-intervention outcomes, $Y_{i,t_0}(0), \dots, Y_{i,1}(0)$. Under Assumption 3, the quantity $Y_{i,t_0+k|t_0}(0)$ can be identified from available data:

$$f_{Y_{i,t_0+1}(0)|\mathcal{I}_{t_0}, \mathbf{X}_{i,t_0+1}}(y_{i,t_0+1}(0)|\mathcal{I}_{t_0}, \mathbf{X}_{i,t_0+1}) = f_{Y_{i,1}(0)|\mathcal{I}_0, \mathbf{X}_{i,1}}(y_{i,t_0+1}(0)|\mathcal{I}_{t_0}, \mathbf{X}_{i,t_0+1}). \quad (1)$$

This means that, if we know the density of the outcome absent the intervention at time $t = 1$ (conditioning on the information up to $t = 0$) and we assume that the functional form of the conditional outcome is invariant to time translation (conditional stationarity), then we would also know the outcome density at time $t = t_0 + 1$ provided we condition on the information set up to $t = t_0$. We also remark that the first part of Assumption 2 is implicit in Assumption 3. This is because if anticipatory effects were present, they would modify the distribution of pre-intervention outcomes, thereby invalidating the assumption of conditional stationarity. Therefore, under both Assumptions 2 and 3, from the conditional density (1) and the information set \mathcal{I}_{t_0} , we can retrieve the conditional

expectation $Y_{i,t_0+1|t_0}(0) = E[Y_{i,t_0+1}(0)|\mathcal{I}_{t_0}, \mathbf{X}_{i,t_0+1}]$. Similarly, at time $t = t_0 + 2$ we have,

$$\begin{aligned}
& f_{Y_{i,t_0+2}(0)|\mathcal{I}_{t_0}, \mathbf{X}_{i,t_0+1}, \mathbf{X}_{i,t_0+2}}(y_{i,t_0+2}(0)|\mathcal{I}_{t_0}, \mathbf{X}_{i,t_0+1}, \mathbf{X}_{i,t_0+2}) = \\
& = \int f_{Y_{i,t_0+2}(0), Y_{i,t_0+1}(0)|\mathcal{I}_{t_0}, \mathbf{X}_{i,t_0+1}, \mathbf{X}_{i,t_0+2}}(y_{i,t_0+2}(0), y_{i,t_0+1}(0)|\mathcal{I}_{t_0}, \mathbf{X}_{i,t_0+1}, \mathbf{X}_{i,t_0+2}) dy_{i,t_0+1} \\
& = \int f_{Y_{i,t_0+2}(0)|\mathcal{I}_{t_0+1}, \mathbf{X}_{i,t_0+2}}(y_{i,t_0+2}(0)|\mathcal{I}_{t_0+1}, \mathbf{X}_{i,t_0+2}) \\
& \quad \cdot f_{Y_{i,t_0+1}(0)|\mathcal{I}_{t_0}, \mathbf{X}_{i,t_0+1}}(y_{i,t_0+1}(0)|\mathcal{I}_{t_0}, \mathbf{X}_{i,t_0+1}) dy_{i,t_0+1} \\
& = \int f_{Y_{i,t_0+1}(0)|\mathcal{I}_{t_0}, \mathbf{X}_{i,t_0+1}}(y_{i,t_0+2}(0)|\mathcal{I}_{t_0+1}, \mathbf{X}_{i,t_0+2}) \\
& \quad \cdot f_{Y_{i,t_0+1}(0)|\mathcal{I}_{t_0}, \mathbf{X}_{i,t_0+1}}(y_{i,t_0+1}(0)|\mathcal{I}_{t_0}, \mathbf{X}_{i,t_0+1}) dy_{i,t_0+1}.
\end{aligned}$$

The last equality follows directly from Assumption 2, as we are assuming that the functional form of $Y_{i,t_0+2}(0)$ given the new information set $\mathcal{I}_{t_0+1} = \{Y_{i,t_0+1}(0), \mathbf{X}_{i,t_0+1}, \mathcal{I}_{t_0}\}$ is the same as the functional form of $Y_{i,t_0+1}(0)$ given the information set \mathcal{I}_{t_0} . Since we proved that the latter is identifiable (recall Equation (1)), also the conditional density

$f_{Y_{i,t_0+2}(0)|\mathcal{I}_{t_0}, \mathbf{X}_{i,t_0+1}, \mathbf{X}_{i,t_0+2}}(y_{i,t_0+2}(0)|\mathcal{I}_{t_0}, \mathbf{X}_{i,t_0+1}, \mathbf{X}_{i,t_0+2})$ can be identified from observed data. The proof for a generic time $t_0 + k$ follows analogously by induction. Finally, from Definitions 1 and 2 we have that both the ATE and the CATE are aggregations of individual point effects. Since we have just shown that under Assumptions 2 and 3 the unit-level effect τ_{i,t_0+k} can be identified from available data, its average across N units is also identified. This logic extends to the temporal average effects in Definition 3, as the unit-level effects are identifiable for any strictly positive integer $k = 1, \dots, T - t_0$.

2.3 Modeling assumptions

Our method, whose implementation is detailed in Section 3, starts by running several ML algorithms on pre-treatment data and then selects the one producing the most accurate forecasts. Therefore, since it is not possible to know in advance which ML method will be selected, we maintain the notation as general as possible.¹⁴ Denote with $\mathcal{X}_{i,t-1}^{(q)} = \{\mathbf{X}_{i,t-1}, \dots, \mathbf{X}_{i,t-q}\}$ the set of the past q lags of the covariates up to time $t - 1$ and indicate with $\mathcal{Y}_{i,t-1}^{(p)} = \{Y_{i,t-1}(0), \dots, Y_{i,t-p}(0)\}$ a set of the past p lags of $Y_{i,t}(0)$ up to time $t - 1$ with $p, q = 1, \dots, t - 1$.

To estimate the causal quantities outlined in Section 2.2, two additional assumptions are required. We emphasize that such assumptions are not particularly restrictive, as the MLCM is designed to be highly flexible.

First, we assume that the potential outcome absent the policy is as follows,

$$Y_{i,t}(0) = f\left(\mathcal{Y}_{i,t-1}^{(p)}(0), \mathbf{X}_{i,t}, \mathcal{X}_{i,t-1}^{(q)}\right) + \epsilon_{i,t} \quad (2)$$

where $f(\cdot)$ is some flexible function of the past lags of the outcome, the contemporaneous covariates, and the past lags of covariates, and $\epsilon_{i,t}$ is the error term. Notice that model (2) assumes poolability, i.e., once we account for a highly predictive set of covariates and include temporal dynamics through lagged outcomes, the residual component is essentially random noise.¹⁵ We posit this assumption can

¹⁴We believe this is an advantage over most existing approaches in the causal ML literature: while [Carvalho et al. \(2018\)](#) and [Masini and Medeiros \(2021\)](#) focus on LASSO and [Wager and Athey \(2018\)](#) adopt tree-based methods, the MLCM is flexible and can easily adapt to different data-generating processes. A notable exception in this context is the synthetic learner proposed by [Viviano and Bradic \(2023\)](#). In contrast to their technique, our method is based on a horse-race competition between several alternative ML algorithms, whereas the synthetic learner relies on an ensemble procedure that combines various estimators (not only ML ones).

¹⁵For panel data studies with small T and large N , it is usual to pool the observations ([Baltagi, 2008](#)).

be met in practice by using a subset of very predictive covariates out of a larger initial set selected *ex ante* on the basis of domain knowledge. This approach ensures that major sources of heterogeneity among units are effectively addressed. In cases where the researcher also wants to account for unobserved heterogeneity by adding units' fixed-effects, the covariate set could be augmented with dummy variables, as it is frequently done in the panel literature with the Least Squares Dummy Variable estimator (Verbeek, 2017), or by adopting more recent approaches based on sufficient representations for categorical variables (Johannemann et al., 2019). In addition, we remark that model 2 does not assume stationarity of the time series in the panel dataset, as the MLCM only relies on conditional stationarity. The highly flexible and entirely data-driven panel CV approach is designed to accurately capture any temporal dynamics present during the pre-intervention period and then extend these patterns into the future. As long as the dynamics do not change due to co-occurring policies or other unforecastable shocks, the projected trajectory estimates the counterfactual outcome in the absence of the intervention.¹⁶

We also assume that the intervention produces an additive effect on the potential outcomes, i.e.,

$$Y_{i,t}(1) = Y_{i,t}(0) + \epsilon_{i,t}.$$

This is not a restrictive assumption, since it holds after a suitable transformation of the data. For example, we can start from a multiplicative effect and then apply a logarithmic transformation to recover an additive structure.

2.4 Estimators

In this subsection, we introduce estimators of the causal quantities defined in Section 2.2. Note that we propose estimators of causal effects at a general time point $t_0 + k$ after the intervention without relying on untreated units. This requires a multi-step ahead imputation of the counterfactual potential outcomes, which introduces certain challenges that will be addressed below. Recalling Definition 1, we first define an estimator for the counterfactual outcome in the absence of the policy.

Definition 4 *Let $Y_{i,t}(0)$ follow from Equation (2). For any strictly positive integer k , an estimator of the counterfactual outcome in the absence of the intervention at time $t_0 + k$, given the information available up to time t_0 and the contemporaneous covariates is,*

$$\begin{aligned} \hat{Y}_{i,t_0+k|t_0} &= \mathbb{E}[Y_{i,t_0+k} | \mathcal{I}_{t_0}, \mathbf{X}_{i,t_0+k}] \\ &= \mathbb{E} \left[f \left(\mathcal{Y}_{i,t_0+k-1}^{(p)}(0), \mathbf{X}_{i,t_0+k}, \mathcal{X}_{i,t_0+k-1}^{(q)} \right) \right] \\ &= \hat{f} \left(\mathcal{Y}_{i,t_0+k-1}^{(p)}(0), \mathbf{X}_{i,t_0+k}, \mathcal{X}_{i,t_0+k-1}^{(q)} \right). \end{aligned} \quad (3)$$

In the above expression, $\hat{f}(\cdot)$ denotes the predicted value of $f(\cdot)$. Notice that when $k = 1$, we would be focusing on a special setting with a single post-intervention period. In such a case, the prediction of $\hat{Y}_{i,t_0+1|t_0}$ is straightforward, as it only depends on pre-treatment values of the outcome and the covariates and, possibly, some contemporaneous covariates. Instead, when $k > 1$ and we want to

¹⁶More generally, in our setting of interest, a short panel with small T and large N, non-stationarity is not an issue of particular concern (Baltagi, 2008). Nevertheless, as we will show below, the simulation results reported in Appendix D demonstrate that even in the case of an explosive autoregressive coefficient (i.e., when the coefficient of the past lag of the outcome Y_{t-1} is set at $\phi = 1.2$), both the bias and the coverage rates of the MLCM are in line with the results obtained for stationary processes (i.e., when $\phi = 0.8$).

include the past p lags of the outcome as in Equation (2), $Y_{i,t_0+k}(0)$ would depend on post-treatment counterfactual outcomes. To understand why, consider the case where $k = 2$ and $p = 1$: following Definition 4, the estimation of $\widehat{Y}_{i,t_0+2|t_0}(0)$ has to be made conditionally on the information set up to time t_0 but under Equation (2) we have $\mathcal{Y}_{i,t_0+1}^{(1)}(0) = Y_{i,t_0+1}(0)$, meaning that the potential outcome absent the policy is function of the unobserved outcome at time $t_0 + 1$. To solve this challenge, we have two options: i) we only rely on pre-intervention outcomes by imposing that $f(\cdot)$ contains the past p lags of the outcome up to time t_0 , i.e., $Y_{i,t_0+k}(0) = f\left(\mathcal{Y}_{i,t_0}^{(p)}(0), \mathbf{X}_{i,t_0+k}, \mathcal{X}_{i,t_0+k}^{(q)}\right) + \epsilon_{i,t_0+k}$; ii) we recursively condition on the predicted counterfactual. While the first option appears artificial (e.g., when $k = 2$, assuming that $Y_{i,t_0+2}(0)$ depends on its previous lags up to $Y_{i,t_0}(0)$ is equivalent to assuming that in an autoregressive model $Y_{i,t}$ depends on $Y_{i,t-2}$ but not on $Y_{i,t-1}$), the second option is perfectly viable under Assumption 3: if the conditional distribution of the potential outcome in the absence of the intervention does not change with time translations, $\widehat{Y}_{i,t_0+1}(0)$ is a reliable estimator of the potential outcome in the absence of the intervention and it can be used for the prediction of $\widehat{Y}_{i,t_0+2|t_0}(0)$. Notice that the same two options are available when we rely on covariates that could be impacted by the intervention: if we assume that such covariates follow Equation (2), we can forecast counterfactual values of $\widehat{\mathbf{X}}_{i,t_0+k|t_0}(0)$ and incorporate them into the prediction of $\widehat{Y}_{i,t_0+k|t_0}(0)$.

Recall that under Assumption 2, we observe $Y_{i,t} = Y_{i,t}(1)$ at time $t > t_0$, and, as we have the entire population, it is a fixed quantity. Then, the estimator for the unit-level causal effect at time $t_0 + k$ is,

$$\widehat{\tau}_{i,t_0+k} = Y_{i,t_0+k} - \widehat{f}\left(\mathcal{Y}_{i,t_0+k-1}^{(p)}(0), \mathbf{X}_{i,t_0+k}, \mathcal{X}_{i,t_0+k-1}^{(q)}\right). \quad (4)$$

Building on Equations (3) and (4), the next definition summarizes the causal effect estimators under the MLCM approach.

Definition 5 For any positive integer k , $Y_{i,t_0+k} = Y_{i,t_0+k}(1)$ is the observed outcome in the post-intervention period under Assumption 2. A finite-sample estimator for ATE at time $t_0 + k$ under model (2) is,

$$\widehat{\tau}_{t_0+k} = \frac{1}{N} \sum_{i=1}^N \widehat{\tau}_{i,t_0+k} = \frac{1}{N} \sum_{i=1}^N \left(Y_{i,t_0+k}(1) - \widehat{f}\left(\mathcal{Y}_{i,t_0+k-1}^{(p)}(0), \mathbf{X}_{i,t_0+k}, \mathcal{X}_{i,t_0+k-1}^{(q)}\right) \right). \quad (5)$$

A finite-sample estimator for group CATE at time $t_0 + k$ is,

$$\widehat{\tau}_{t_0+k}(g) = \frac{1}{N_g} \sum_{i:G_{i,t_0+k}=g} \widehat{\tau}_{i,t_0+k}. \quad (6)$$

Finally, estimators for the temporal average ATE and CATE are, respectively,

$$\widehat{\tau} = \frac{1}{T - t_0} \sum_{k=1}^{T-t_0} \widehat{\tau}_{t_0+k} \quad (7)$$

$$\widehat{\tau}(g) = \frac{1}{T - t_0} \sum_{k=1}^{T-t_0} \widehat{\tau}_{t_0+k}(g).$$

Inference on the estimated causal effects defined above is conducted using block-bootstrap. Refer to Appendix A for a detailed description of the block-bootstrap algorithms used to derive confidence intervals for ATE and CATEs. Finally, Appendix B reports an overview of a selection of supervised

ML models (namely, those that we employ in both the simulation of section 3.3 and the empirical application of section 4) which can be implemented within the MLCM estimation framework.

3 The Machine Learning Control Method

3.1 Departures from the standard machine learning approach

Supervised ML techniques primarily aim to minimize the out-of-sample prediction error, generalizing well on unseen data. The degree of flexibility is the result of a trade-off: increased flexibility can enhance in-sample fit but may diminish out-of-sample fit due to overfitting. ML algorithms tackle this trade-off by relying on empirical tuning to choose the optimal level of complexity.

The standard ML approach is to randomly split the sample into two sets, containing, for instance, 2/3 and 1/3 of observations. One then uses the first set to train ML algorithms (training set) and the second to test them (testing set). This introduces a “firewall” principle: none of the data involved in generating the prediction function is used to evaluate it (Mullainathan and Spiess, 2017). The out-of-sample performance of the model on the unseen (held-out) data of the testing set can be considered a reliable measure of the “true” performance on future data. In order to solve the bias-variance trade-off and prevent overfitting, one can rely on automatic tuning using tools such as random k-fold CV on the training sample to select the best-performing values of the tuning parameters in terms of an *a priori* defined metric, such as the Mean Squared Error (MSE).

We depart from this standard ML routine and reorient it towards the counterfactual forecasting goal. First, we do not randomly split the data, but we train, tune, and evaluate the models only on the pre-treatment data (Design Stage); then, we use the final selected model to forecast counterfactual post-treatment outcomes. In this forecasting perspective, the unseen data on which the ML models must generalize well are not the outcomes of different units (as in typical out-of-sample prediction tasks), but future observations of the outcome for the same set of units employed to train the models. Stated differently, the aim is to make ML models learn as best as possible the pre-intervention outcome trend for each treated unit, so as to predict the best possible counterfactual outcome under the no-treatment scenario. The key implication of this unconventional ML setup is the shift in focus: the primary concern becomes ensuring unbiasedness in forecasts, rather than focusing only on forecast accuracy.

Second, and related, we do not carry out hyperparameter tuning and model selection with random k-fold CV. The panel dimension, in fact, creates an additional challenge regarding how to exactly implement CV, because standard CV does not account for the temporal structure of the data (Arkhangelsky and Imbens, 2023). To address this challenge, we introduce a resampling technique suited for forecasting tasks on panel data—panel CV—which is fully described below.

Finally, a key concern in ML regards the trade-off between accuracy and interpretability. Such a trade-off is relevant when ML is used for tasks that take into consideration transparency and interpretability aspects. In the case of the MLCM, we argue that preserving transparency is important because higher interpretability of the estimated counterfactuals bolsters the credibility of the proposed approach (Abadie, 2021). Since our method can be used with any supervised ML routine, users should decide on the basis of a comparative performance assessment across a mix of models characterized by different layers of complexity by carefully balancing any improvements in performance from complex models against the loss of interpretability that comes with their use.

3.2 Implementation

The implementation of the MLCM requires ten empirical steps, divided into the Design Stage and the Analysis Stage. The full process is summarized in Box 1 and described in detail below.

Box 1: MLCM implementation	
Preliminary	
0. Data splitting. Split the full sample based on the treatment date: employ only pre-treatment data throughout the Design Stage; use post-treatment data only for estimating causal effects in the Analysis Stage.	
Design Stage	
1. Algorithm selection. Select one or more supervised ML algorithms.	
2. Principled input selection. Build a large initial dataset on the basis of domain knowledge. To maximize forecasting performances, it is possible to use feature engineering, feature selection, and heuristic rules to pre-process the data and select a subsample of the most relevant predictors.	
3. Panel cross-validation. For each selected algorithm, tune hyperparameters via panel CV (see Figure 1 for the case of one-step ahead forecasts).	
4. Performance assessment. Assess average performance metrics (e.g., MSE) for all the selected algorithms and check what is the best-performing version of the MLCM.	
5. Diagnostic and placebo tests. Implement a battery of diagnostic and placebo tests to bolster the credibility of the research design.	
Analysis Stage	
6. Final model selection. On the basis of the comparative performance assessment in the Design Stage, pick the best-performing model and use that for the Analysis Stage. Start by re-training the model on the full pre-treatment sample using the hyperparameter(s) selected in the Design Stage.	
7. Counterfactual forecasting. For each unit i , forecast the post-treatment counterfactual outcome $\hat{Y}_{i,t_0+k t_0}$. In case of a large-scale shock affecting important covariates, either rely solely on their past lags or repeat steps 1–6 to forecast $\hat{\mathbf{X}}_{i,t_0+k t_0}(0)$ and use these values to improve the forecast of $\hat{Y}_{i,t_0+k t_0}$.	
8. Estimation of treatment effects. For each unit i , estimate the individual treatment effect in Equation (4) by taking the difference between the observed post-treatment outcome Y_{i,t_0+k} and the ML-generated potential outcome $\hat{Y}_{i,t_0+k t_0}$. Estimate other causal estimands, such as the ATE from Equation (5) or the temporal ATE from Equation (7), by aggregating the individual estimates.	
9. Treatment effect heterogeneity. To uncover heterogeneity, data-driven CATEs can be estimated as in Equation (6) via a regression tree analysis with the individual treatment effects as the outcome variable and a set of exogenous predictors potentially associated with treatment effect heterogeneity.	
10. Inference. Compute standard errors for the ATE and CATEs via block-bootstrap.	

In the Design Stage, the first step involves the selection of supervised ML algorithms that will play the horse-race of performance testing on the pre-treatment data.¹⁷ In the second step, we recommend deploying some tweaks involving feature pre-selection and engineering drawing from consolidated practices in applied predictive modeling (Kuhn and Johnson, 2013). A crucial aspect of this pre-processing is the strategy for selecting predictors. There are two main schools of thought: those who advocate

¹⁷It is possible to stack several different ML algorithms and form complex ensemble learners, but we refrain from their use because, as stated above, we deem it important to retain some degree of transparency in counterfactual building.

for purely data-driven selection argue that one should build a dataset as large as possible, and then let the algorithm autonomously decide which variables matter for the forecasting task. Others stress the importance of subject matter knowledge: the researcher should select *ex ante* the relevant predictors, and then feed only those to the algorithm. The underlying rationale is that subject matter knowledge can separate meaningful from irrelevant information, eliminating detrimental noise and enhancing the underlying signal (Kuhn and Johnson, 2013). We propose a hybrid approach: build a large initial dataset on the basis of domain knowledge, then adopt preliminary and data-driven variable selection criteria to drop non-informative predictors.

As outlined in the causal framework, counterfactual forecasting is carried out by using an information set mainly comprising lagged values of outcomes and covariates. However, determining the optimal number of lags to include is an empirical question. We recommend including at least two lagged values of both outcomes and covariates, and then using a data-driven approach to select a sub-sample of the most relevant features. The latter step allows for a reduction of the risk of overfitting and degradation of forecasting performances as well as facilitating interpretability. Finally, remember that feature engineering and data pre-processing matter too because how the predictors enter into the model is also important (Kuhn and Johnson, 2013).

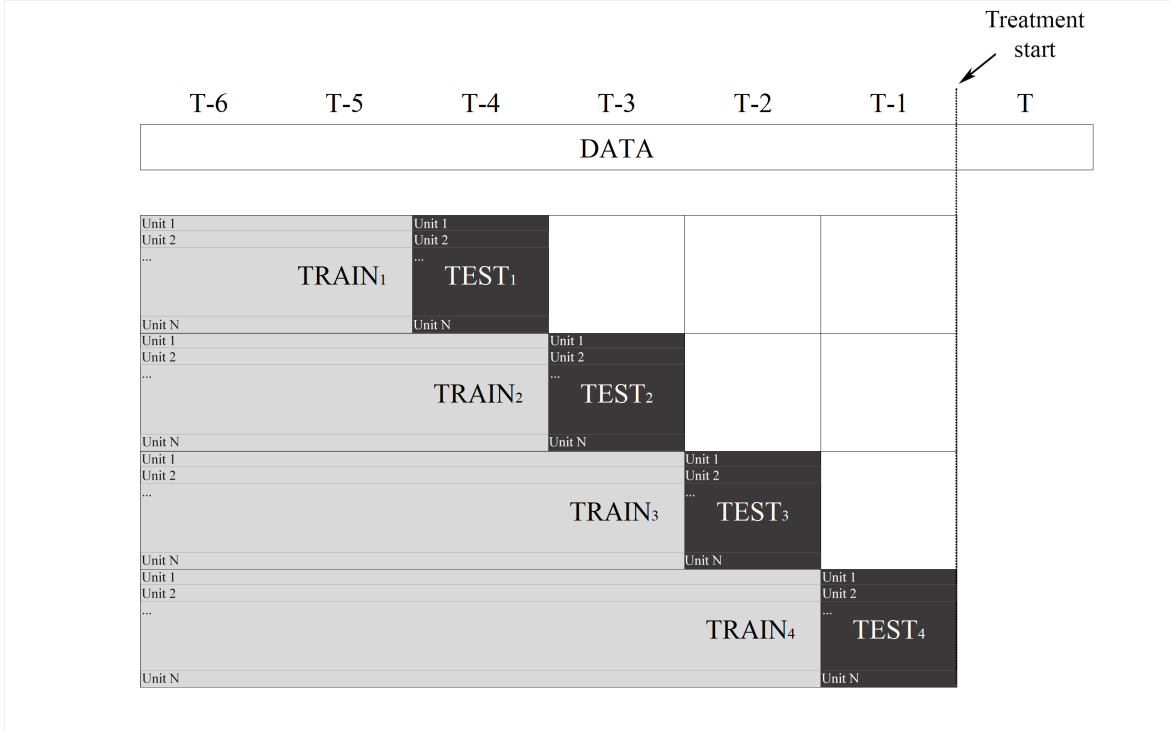
To carry out model selection and validation on the pre-treatment sample, we propose a panel CV approach. In our setting, using an alternative CV procedure is necessary since ML methods do not natively handle longitudinal data and are designed for predicting rather than forecasting. Our panel CV approach adapts time series CV based on expanding training windows to a panel setting.¹⁸ The intuition—for the case of one-step ahead forecasts, but the routine is easily adapted to multi-step ahead forecasts—is provided in Figure 1 and constitutes an adaptation from Hyndman and Athanasopoulos (2021).

In short, we establish cutoff points in the temporal dimension as $\{t_0 - s, t_0 - s + 1, \dots, t_0 - 1\}$, with s denoting a strictly positive integer such that $t_0 - s \geq 1$. At the first CV step, these cutoffs delineate a training set $\mathcal{T}_1 = \{Y_{i,t} : t = 1, \dots, t_0 - s\}$ and a validation set $\mathcal{V}_1 = \{Y_{i,t} : t = t_0 - s + 1\}$. At the second CV step, the training set becomes $\mathcal{T}_2 = \{Y_{i,t} : t = 1, \dots, t_0 - s + 1\}$ and the validation set $\mathcal{V}_2 = \{Y_{i,t} : t = t_0 - s + 2\}$ and so on, until the final CV step, where the validation set includes the observations in the last time period before the intervention. This sequential procedure ensures that, for each unit, there are no “future” observations in the training set and no “past” observations in the validation set. At each step, the parameters’ values yielding the best predictive performance in the validation step (e.g., those minimizing the MSE) are stored and then averaged across all CV steps. This also provides summary measures of average model performance on the pre-treatment data, which can be screened to select the winner of the horse-race.

To provide evidence about internal validity, we suggest running diagnostic checks (e.g., showing that the distribution of the pre-treatment forecasting errors is approximately Gaussian and centered around zero) as well as placebo tests, which have become a key device for assessing the credibility of research designs in observational settings (Eggers et al., 2021). Following Liu et al. (2022), panel placebo tests can be implemented by hiding one or more periods of observations right before the onset of the treatment and using a model trained on the rest of the pre-treatment periods to predict the untreated outcomes of the held-out period(s). If the identifying assumptions are valid, the differences between the observed and forecast outcomes in those periods should be close to zero. Importantly,

¹⁸Here we use an expanding window (as we are in a short-panel setting), but the procedure can also be implemented using a rolling window approach, which might be more appropriate in specific cases (e.g., with long panels or non-stationarity of the outcome).

Figure 1: Panel cross-validation (one-step ahead forecasting). Note: this procedure is carried out using exclusively pre-treatment data. Light gray observations form the training sets; dark gray ones constitute the test sets. All the training windows also include past outcomes in the set of predictors.



given that we estimate unit-level treatment effects, we are able to do more than just show that the average differences are close to zero (the standard practice in most event-study designs) and test whether most unit-level placebo differences are close to zero. The Design Stage thus ends with a battery of performance, diagnostic, and placebo tests.

The Analysis Stage starts with final model selection and training: on the basis of the comparative performance assessment in the Design Stage, pick the best-performing model, re-train it on the full pre-treatment sample (using the hyperparameter values obtained in the Design Stage), then use it to forecast counterfactual outcomes in the post-intervention period. Once that is done, treatment effects for each unit are given by the difference between the post-treatment observed data and the corresponding ML-generated counterfactual forecasts. The ATE is the average of the individual effects.

When dealing with a single post-intervention period, step 7 of the Analysis Stage is straightforward. However, when performing a multi-step ahead forecast using a data-driven ML routine, one must take special care to avoid including post-treatment outcomes in the prediction. To achieve this, we adopt the following procedure: we first forecast the counterfactual outcome absent the policy at time $t_0 + 1$ (by relying only on pre-treatment information) and obtain an estimate of $\hat{Y}_{i,t_0+1|t_0}$. Then we proceed one step ahead, by including $\hat{Y}_{i,t_0+1|t_0}$ in the past information set and using it to forecast $\hat{Y}_{i,t_0+2|t_0}$. We recursively substitute the forecasted value until we reach the last time point, $\hat{Y}_{i,t_0+T|t_0}$.¹⁹ Furthermore, note that the same procedure can be applied to forecast post-treatment values of important covariates affected by the intervention. Like in the case of past outcomes (see Section 2.4), there are two options for handling covariates that could be impacted by the intervention: either we impose that $f(\cdot)$ contains the past q lags of \mathbf{X}_{i,t_0+k} up to t_0 , or we assume that such covariates follow Equation (2) and use the

¹⁹This is analogous to what is typically done in the usual time series setting. Consider for example an AR(1) process: $y_t = \phi y_{t-1} + \epsilon_t$, with $|\phi| < 1$. The 1-step ahead forecast is given by $y_{t+1|t} = \mathbb{E}[y_{t+1}|\mathcal{I}_t] = \phi \mathbb{E}[y_t|\mathcal{I}_t] = \phi y_t$; the 2-step ahead forecast is readily computed from the forecasted value $y_{t+1|t}$, i.e., $y_{t+2|t} = \mathbb{E}[y_{t+2}|\mathcal{I}_t] = \phi \mathbb{E}[y_{t+1}|\mathcal{I}_t] = \phi^2 y_t$.

ML algorithms and the panel CV routine to forecast counterfactual values of $\widehat{\mathbf{X}}_{i,t_0+k|t_0}(0)$, which we can then incorporate into the prediction of $\widehat{Y}_{i,t_0+k|t_0}$.

Next, data-driven CATEs are computed via a regression tree analysis on the full sample of estimated treatment effects. Specifically, this approach uses the estimated treatment effects as the outcome variable, regresses them on many potentially associated variables, and lets the algorithm pick the main predictors and their critical thresholds. The resulting tree reports the group-average treatment effects for all units in each terminal node. As for causal trees and forests (Athey and Imbens, 2016; Wager and Athey, 2018), this data-driven search for heterogeneity of causal effects removes a major degree of discretion because the researcher can only select the set of covariates that can be used by the tree to build the subgroups. However, the two approaches differ regarding both purpose and implementation: our data-driven technique is a post-estimation approach aimed at automatically recovering and visualizing the relevant heterogeneity dimensions, while causal trees and forests are counterfactual methods for the direct estimation of heterogeneous treatment effects, which they achieve by leveraging control units. Moreover, we are not interested in the out-of-sample performance of the regression tree, but in retrieving CATEs for the entire population of interest. To this end, there is no need either to split the sample into training and testing sets or to prune the tree by adjusting the complexity parameter.

Finally, standard errors and confidence intervals for the ATE and CATEs are estimated through the block-bootstrap approach described in Appendix A.

3.3 Simulation study

To investigate the performance of the MLCM in detecting average treatment effects in panel datasets, we performed an extensive simulation study using different data-generating processes (linear and non-linear) and various combinations of pre- and post-intervention periods. In further detail, we generated 1,000 panel datasets, each consisting of 400 units and $T = 7$ or 12 time periods, according to the following two models,

$$Y_{i,t}(0) = \phi Y_{i,t-1}(0) + \mathbf{X}_{i,t-1}\boldsymbol{\beta} + \epsilon_{i,t} \quad (\text{Linear})$$

$$Y_{i,t}(0) = \sin\{\phi Y_{i,t-1}(0) + \mathbf{X}_{i,t-1}\boldsymbol{\beta}\} + \epsilon_{i,t} \quad (\text{Non-Linear})$$

where: the error term $\epsilon_{i,t}$ is generated from a Normal distribution with standard deviation $\sigma_\epsilon = 2$, i.e., $\epsilon_{i,t} \sim N(0, 2)$, $\phi = 0.8$ is the autoregressive coefficient, $\boldsymbol{\beta} = (\beta^{(1)}, \dots, \beta^{(11)})'$ is a $m \times 1$ vector of coefficients and $\mathbf{X}_{i,t-1} = (\mathbf{X}_{i,t-1}^{(1)}, \dots, \mathbf{X}_{i,t-1}^{(11)})$ is a $1 \times m$ vector of 11 predictors, both continuous and categorical, also containing interaction terms and correlated regressors. We allowed the covariates to vary in time and across units in the dataset by adding, respectively, a random term ν_t (which, as will become clear later, varies for different covariates) and a random term $u_i \sim N(1, 1)$. The latter term adds variability (and thus, heterogeneity) between the units. In particular, the covariates are generated as follows: $\mathbf{X}_{i,t}^{(1)} = 0.1t + u_i + \nu_t^{(1)}$, $\nu_t^{(1)} \sim N(0, 1)$, $\mathbf{X}_{i,t}^{(2)} = 0.1t + u_i + \nu_t^{(2)}$, $\nu_t^{(2)} \sim N(0, 0.2)$, $\mathbf{X}_{i,t}^{(3,4,5)} = u_i + \nu_t^{(3,4,5)}$, $\nu_t^{(3,4,5)} \sim MVN(0, \Sigma)$, $\mathbf{X}_{i,t}^{(6)} = u_i - \nu_t^{(6)}$, $\nu_t^{(6)} \sim N(0, 1)$, $\mathbf{X}_{i,t}^{(7)} = (0.1t + \nu_t^{(1)})^2 + u_i + \nu_t^{(7)}$, $\nu_t^{(7)} \sim N(0, 0.2)$, $\mathbf{X}_{i,t}^{(8)} \in \{0, 1\}$, $\mathbf{X}_{i,t}^{(9)} \in \{1, 2, 3\}$, $\mathbf{X}_{i,t}^{(10)} = \mathbf{X}_{i,t}^{(3)} \cdot \mathbf{X}_{i,t}^{(9)}$, $\mathbf{X}_{i,t}^{(11)} = \mathbf{X}_{i,t}^{(2)} \cdot \mathbf{X}_{i,t}^{(8)}$.²⁰ These choices regarding the data-generating process for the covariates included in our simulation study are

²⁰The variance-covariance matrix of the multivariate normal distribution used to generate covariates 3-5 is set to $\Sigma = \begin{bmatrix} 1 & .5 & .7 \\ .5 & 1 & .3 \\ .7 & .3 & 1 \end{bmatrix}$. Notice that, to put the ML algorithms under further stress, the covariance between $\mathbf{X}_{i,t}^{(3)}$ and $\mathbf{X}_{i,t}^{(5)}$ is 0.7 so the two variables are highly correlated but $\mathbf{X}_{i,t}^{(3)}$ is ten times more important (in terms of coefficient) than $\mathbf{X}_{i,t}^{(5)}$.

driven by the goal of mirroring real-world empirical settings where the methodology might be applied. In addition, to better reflect a typical real-world scenario where only a subset of covariates is relevant, we set certain coefficients to zero: specifically, $\beta^{(1)}$, $\beta^{(8)}$, and $\beta^{(9)}$. The remaining coefficients are generated as follows: $\beta^{(2)} = \beta^{(6)} = \beta^{(10)} = 2$, $\beta^{(3)} = \beta^{(7)} = 1$, $\beta^{(4)} = 2.5$, $\beta^{(5)} = 0.1$ and $\beta^{(11)} = 1.5$. We also remark that, for computational reasons, in this simulation study we focus on a low-dimensional set of covariates. However, the MLCM is particularly well-suited for data-rich environments and sparse settings with hundreds or thousands of possible covariates. In this regard, the simulation results provided here should be interpreted as conservative evidence regarding the performance of the MLCM in real-world settings. Finally, we assume exogeneity of the predictors in both the pre- and post-intervention periods (Assumption 2). Table 1 below provides an overview of the generated datasets.

Table 1: First 9 observations from one of the datasets generated during the simulation study

Time	ID	Y	X ⁽¹⁾	X ⁽²⁾	X ⁽³⁾	X ⁽⁴⁾	X ⁽⁵⁾	X ⁽⁶⁾	X ⁽⁷⁾	X ⁽⁸⁾	X ⁽⁹⁾	X ⁽¹⁰⁾	X ⁽¹¹⁾
1	1	16.57	1.71	0.9	1.38	3.61	3.03	0.42	1.09	0	1	1.38	0
2	1	43.62	1.62	1.53	2.4	3.33	3.73	1.14	1.24	0	3	7.19	0
3	1	73.62	2.83	1.71	3.13	3.44	3.99	3.89	3.37	1	1	3.13	1.71
4	1	89.04	1.16	1.91	1.53	3.35	2.25	1.14	1.25	1	3	4.58	1.91
5	1	170.17	2.61	1.62	1.99	1.47	3.46	1.23	3.79	0	2	3.98	0
6	1	153.05	1.43	1.63	1.3	3.3	3.2	1.22	1.65	0	1	1.3	0
7	1	133.43	0.3	1.8	0.46	1.43	3.38	1.32	1.14	1	3	1.38	1.8
1	2	16.88	1.42	1.14	0.23	2.93	3	0.6	2.11	1	3	0.7	1.14
2	2	45.33	1.66	1.75	2.94	3.2	3.57	0.56	1.13	0	2	5.87	0

At the last three time points (e.g., $T = 5, 6$, and 7 in Table 1), we included a fictional intervention that increases the outcome for each unit by 2 standard deviations at time $t_0 + 1$, 1.5 standard deviations at time $t_0 + 2$, and 1 standard deviation at time $t_0 + 3$. In other words, the intervention has a decreasing effect over time. We made this choice because adding a unit-specific component in the covariates generates heterogeneity; therefore, the scale of each Y_i varies across the i 's. We measured the performance of the MLCM in terms of both the bias of the estimated effect from the true impact and the interval coverage. Also note that, under this setup, the number of pre-intervention periods is $t_0 = 4$ when $T = 7$ and $t_0 = 9$ when $T = 12$.

The results are summarized in Table 2 below and show that, across all post-intervention horizons, the MLCM achieves a very low bias. This holds true for both linear and non-linear model specifications. The bias tends to decrease when the number of pre-intervention time periods increases, as more information is present in the data. Nevertheless, the bias at the shortest time period is still very low, which reinforces our belief that the MLCM can be effectively used for short panels. For instance, under the linear specification and $t_0 = 4$, the relative bias increases from 0.2% measured at $t_0 + 1$ to 0.9% measured at $t_0 + 3$. However, by increasing the number of pre-intervention time points, the bias drops at 0.4% even at $t_0 + 3$. We also observe that the relative bias under a linear model specification is much lower than that under the non-linear specification, which was expected since non-linearities are typically more challenging to detect. In any case, the bias under a non-linear model specification is still low (the maximum bias is 4.9% and is measured in the worst-case scenario, i.e., at the third time horizon when the pre-intervention series is very short, $t_0 = 4$).

Similar observations can be made for the interval coverage, which was estimated based on 1,000 block-bootstrap iterations. At the first time horizon after the intervention, the interval coverage is

close or equal to the nominal 95% level for both linear and non-linear model specifications. Then, it tends to slightly decrease as we move further away from the intervention, but remains close to the nominal level for both linear and nonlinear processes.

Overall, these numerical studies demonstrate that the MLCM can achieve forecast unbiasedness and that the coverage of the estimator is high even when considering short pre-intervention windows. The simulation results also suggest that when we are interested in the estimation of causal effects k -step ahead from the treatment, having a greater number of pre-intervention periods further mitigates the bias, both under linear and non-linear data-generating processes.

Table 2: Simulation results for the linear and non-linear model specifications

		1st Post-intervention period ($t_0 + 1$)							
		Linear				Non-Linear			
Pre-int.	Bootstrap	True ATE	Bias	Rel. Bias	Coverage	True ATE	Bias	Rel. Bias	Coverage
4	block	74.24	0.14	0.002	0.94	4.06	0.10	0.024	0.95
9	block	93.56	0.10	0.001	0.95	4.14	0.10	0.023	0.94
		2nd Post-intervention period ($t_0 + 2$)							
		Linear				Non-Linear			
Pre-int.	Bootstrap	True ATE	Bias	Rel. Bias	Coverage	True ATE	Bias	Rel. Bias	Coverage
4	block	55.68	0.22	0.004	0.92	3.05	0.10	0.031	0.90
9	block	70.17	0.15	0.002	0.91	3.10	0.09	0.031	0.92
		3rd Post-intervention period ($t_0 + 3$)							
		Linear				Non-Linear			
Pre-int.	Bootstrap	True ATE	Bias	Rel. Bias	Coverage	True ATE	Bias	Rel. Bias	Coverage
4	block	37.12	0.33	0.009	0.93	2.03	0.10	0.049	0.93
9	block	46.78	0.19	0.004	0.92	2.07	0.09	0.046	0.93

Notes. These results are obtained under the following scenario: $N = 400$ units, $\phi = 0.8$, and $\sigma_u = 1$, where σ_u is the standard deviation of the random heterogeneity term u_i . In this table, “Pre-int.” denotes the number of pre-intervention periods.

Importantly, in Appendix D, we provide many additional results that show that these key findings remain largely unchanged if we consider alternative data-generating processes for both the outcome variable and the covariates, and if we reduce the number of available units. Notably, when ϕ is set to 1.2 (cf. Table 4 in Appendix D), rather than to 0.8 as in Table 2, i.e., when moving from a stationary to a non-stationary data-generating process with an explosive autoregressive coefficient for the lag of the outcome variable, the MLCM exhibits very similar performance.

4 Empirical application

4.1 Background

In the aftermath of the COVID-19 pandemic, the inequality legacy of this unprecedented crisis has emerged as an issue of great policy relevance. The available evidence on income inequality documents a decrease driven by short-run and temporary government compensation policies, which were mostly targeted at the poorest segments of the population (Stantcheva, 2022). Concerning education, instead, recent micro-level evidence (Agostinelli et al., 2022; Battisti and Maggio, 2023; Carlana et al., 2023) shows that school closures had a large, persistent, and unequal effect on learning. The educational gaps caused by the school closures may, in turn, permanently affect the lifetime income possibilities of the current generation of students, with vast repercussions on future inequalities (Werner and Woessmann, 2023). Therefore, it is through the human capital channel that the inequality effects of the pandemic may eventually appear in the medium and long run. It follows that to anticipate

longer-term consequences on income inequality and territorial disparities, it is necessary to gauge the magnitude of educational losses and their distribution across areas.

To our knowledge, there is no granular evidence on the geography of the education effects of the COVID-19 crisis. This is mainly due to econometric challenges caused by the sudden spread of the pandemic across the world, which resulted in the absence of a suitable untreated group. Italy is an important case study, as it ranks among the hardest-hit countries and was the first Western country to impose a strict nationwide lockdown. During the lockdown that began on March 9, 2020, schools across the entire national territory were closed and remained so until the end of the school year. This resulted in Italy ranking among the OECD countries with the highest number of weeks of school closures and distance learning (Battisti and Maggio, 2023). In this setting, the treatment—the COVID-19 shock—simultaneously affected all units.²¹ Therefore, we leverage the MLM.

4.2 Data and implementation

We employ LLM yearly data covering the period from 2013 to 2020. We cover all Italian LLMs except some of the smallest ones for which the education data are unavailable due to privacy protection, for a total of 579 LLMs (95% of Italian LLMs and over 99% of the Italian population). The dependent variable is the standardized math test score of fifth-grade students referred to the school year started in 2020. Following the approach by Carlana et al. (2023), the math score is standardized with respect to its pre-pandemic mean. This way, the detected treatment effects can be interpreted as deviations from the pre-COVID baseline. We focus on younger students for two reasons: i) learning disruptions earlier in life typically have longer-lasting and more severe effects, so younger children may have been more heavily impacted (Stantcheva, 2022); ii) primary schools were excluded from the heterogeneous school closures involved in the tier system of regional restrictions implemented by the Italian government since the onset of the second wave (November 2020), so the treatment is the same for all units (Assumption 1). The initial pre-treatment information set includes over 150 variables (see Table 11 in Appendix E for a detailed description of the variables). In this set of covariates, we included the first three lags of all the predictors as covariates and three lags of the outcome variable. This implies that we collapse the original 2013–2020 dataset into a dataset covering the period 2017–2020.

We then use a data-driven approach to restrict the information set. More specifically, we follow Athey and Wager (2019) and Basu et al. (2018) and apply a pilot random forest on the pre-treatment data to pick up a subset of the most important predictors according to the importance ranking produced by the forest.²² In order to select the precise number of relevant predictors in a data-driven manner, we include this number as an additional parameter in the subsequent panel CV routine which we employ to tune the hyperparameters of all the selected algorithms (LASSO, Partial Least Squares, stochastic gradient boosting, and random forest, see Appendix B for an overview of these models).²³

²¹We refer to the treatment variable as COVID-19 “shock”, which encompasses both the pandemic and the containment policies, as we aim to capture the total effect of the pandemic, i.e., its direct and indirect effects on educational outcomes. In this regard, in line with previous literature on COVID-19, we consider the restrictive measures, including the lockdown and the school closures, as a manifestation of the pandemic, not as a separate treatment. COVID-related learning losses can originate from many pandemic-induced channels, such as school closures and distance learning, prolonged absence from school due to one or more infections, absence due to parents’ concerns about their children’s health, and many other transmission mechanisms. At the aggregate level, only the overall impact of the pandemic remains discernible.

²²For this preliminary operation, we use default hyperparameter settings that typically perform well with random forests (Athey and Wager, 2019).

²³For all algorithms, we tune the subset of most predictive variables (10, 20 or 30) to be included in the analysis according to the preliminary forest. For LASSO, we tune the penalty parameter (the values from 0.1 to 0.9 with an increase of 0.1 in each run); for PLS, we tune the number of components (all possible values from 1 to the number of variables). For boosting, we tune the number of trees (1,000 or 2,000), the maximum depth of each tree (1 or 2), the minimum number of observations in terminal nodes (5 or 10) and the learning rate (0.001, 0.002 or 0.005); for random forest, we tune the number of variables randomly sampled as candidates at each split (1/2, 1/3 or 1/4 of the number of

The implementation process for this application is reported in Box 2 below, while the outcomes of the empirical analysis are reported in Section 4.3.

Box 2: Estimating the local impact of the COVID-19 shock on education

Preliminary

0. **Data splitting.** We split the full 2017-2020 dataset into two subsets according to the treatment date: 2017-2019 to be used in the Design Stage; 2020 to be used in the Analysis Stage.

Design Stage

1. **Algorithm selection.** We select four supervised ML algorithms: 1) LASSO; 2) Partial Least Squares; 3) stochastic gradient boosting; 4) random forest. As we are agnostic about the functional form of the underlying data-generating process, we opt for a mix of non-linear and linear models.
2. **Principled input selection.** We build an initial LLM dataset with over 150 predictors on the basis of literature insights. From this dataset, we then keep only the most important predictors selected by a preliminary random forest run on the pre-treatment data (see step below).
3. **Panel cross-validation.** For each algorithm, we tune hyperparameters via panel CV, involving iterative estimation on two different training-testing pairs of pre-COVID datasets: i) 2017 training; 2018 testing; ii) 2017-2018 training, 2019 testing.
4. **Performance assessment.** We assess average performance metrics for the four algorithms by comparing average forecasted vs. actual outcomes on the 2018–2019 held-out test data. We then compare the performance of the different MLCM versions.
5. **Diagnostic and placebo tests.** We first check the average distribution of errors with the best-performing model for the 2018-2019 testing sets and then show the map of the unit-level placebo temporal average treatment effects in the pre-COVID period.

Analysis Stage

6. **Final model selection.** On the basis of the comparative performance assessment, we pick the best-performing algorithm (random forest) and re-train it on the full 2017–2019 sample using the hyperparameters cross-validated in the Design stage.
7. **Counterfactual forecasting.** We apply the final model estimated in Step 6 on the post-pandemic data and forecast, for each LLM i , the counterfactual outcome \hat{Y}_{i,t_0+1} .
8. **Estimation of treatment effects.** For each LLM i , we estimate the individual treatment effect by taking the difference between the observed post-COVID outcome Y_{i,t_0+1} and the ML-generated potential outcome \hat{Y}_{i,t_0+1} .
9. **Treatment effect heterogeneity.** We estimate data-driven CATEs via a regression tree analysis with the individual treatment effects as the outcome and a host of potentially relevant predictors associated with the heterogeneity of the education effects.
10. **Inference.** We estimate standard errors for the ATE and CATEs via block-bootstrapping by performing 1,000 bootstrap replications of Steps 6 to 9.

variables), and use a fixed number of 1,000 trees. All candidate hyperparameter values are tested on each testing set.

Note that in this application, due to the ubiquitous nature of this shock, we do not invoke the second part of Assumption 2 (exogeneity of post-treatment covariates) and only include pre-treatment values of time-varying variables and time-invariant predictors in the information set. However, given the unprecedented disruptions brought about by the pandemic and based on institutional and subject matter knowledge, we deem it plausible that any divergence from the forecasted counterfactual in educational outcomes can be attributed exclusively to the COVID-19 shock, and not to other concomitant shocks or policies.²⁴

4.3 Results

4.3.1 Design Stage

Table 3 below reports the average performance—in terms of MSE—of the four selected ML algorithms in forecasting the standardized math test score of fifth-grade students across the pre-treatment test sets (2018 and 2019).

The best-performing MLCM version is the one using the random forest with 1/4 of the number of variables as candidates at each split. Overall, the fully non-linear random forest and boosting fare better than the linear ML methods, suggesting the presence of non-linearities in the data-generating process. Moreover, the non-linear methods outperform LASSO and Partial Least Squares in all cases, and their performance is stronger in the presence of very few variables and less deteriorated by the inclusion of variables with poor predictive power (cf. Table 12 in Appendix E). The optimal number of variables for random forest corresponds to the 20 variables with the highest importance score attributed by the preliminary forest (see Table 13 in Appendix E for a detailed description of these variables).

Importantly, panel CV on pre-treatment period also implicitly allows one to carry out an in-time placebo analysis along the lines of Bertrand et al. (2004) and Liu et al. (2022). In-time placebos are performed on the same pool of treated units where we “fake” that the treatment occurred at time $t_0 - 1$ and use only information up to $t_0 - 1$ to forecast the counterfactuals at time t_0 . As we know what the real values at time t_0 are, we can use the difference between the actual values and the forecasted values to evaluate forecasting accuracy and assess the unbiasedness of our estimator, as well as the distribution and spatial autocorrelation of the residuals. Put simply, we shift the treatment date artificially backward in time and assess the difference with the main estimates.

As reported in the table, the placebo ATEs are indistinguishable from zero and statistically insignificant both in 2018 (ATE: 0.0554, with 95% confidence intervals $(-0.1182; 0.2765)$) and 2019 (ATE: 0.0254, with 95% confidence intervals $(-0.0273; 0.0728)$).²⁵

²⁴There were no educational reforms at the primary school level that could have influenced the standardized math test scores of fifth-grade students in the period under scrutiny.

²⁵The placebo effects remain statistically indistinguishable from zero when using default hyperparameter values. By “default”, we refer to hyperparameters set at central values based on the most predictive variables—specifically, 20 variables with the highest importance scores from the preliminary forest, and 1/3 of the total number of variables as candidates at each split. Similarly, the counterfactual estimates exhibit substantial similarity regardless of whether a preliminary random forest or an alternative preliminary procedure is employed, such as boosting or selecting covariates based solely on the highest absolute correlation coefficients (e.g., the correlation between the counterfactual estimates and those obtained using default hyperparameter values is 0.9985). Detailed results are available upon request.

Table 3: Performance and placebo estimates

Panel A - Performance	
MLCM using:	MSE
LASSO	0.4169
Partial Least Squares	0.4044
Boosting	0.3909
Random Forest	0.3902
Panel B – Placebo estimates	
Time period	Placebo ATE
2018	0.0554 (-0.1182 ; 0.2765)
2019	0.0254 (-0.0273 ; 0.0728)
Temporal average	0.0404

Notes. The panel CV procedure has selected the 20 most predictive variables out of the initial dataset for all methods. In addition, for boosting, it has selected 2,000 trees, 2 as the maximum depth of each tree, 5 as the minimum number of observations in terminal nodes and 0.005 for the learning rate. The other hyperparameters selected are: 0.3 as the penalty parameter (LASSO), 9 as the number of components (PLS), and 6 for the number of variables randomly sampled as candidates at each split (random forest). Lower and upper bounds of placebo ATE estimates refer to the 95% confidence interval and are reported within brackets.

In addition, the unit-level placebo map in Figure 2 depicts the temporal average (for the years 2018 and 2019) individual ‘treatment’ effects estimated with the best-performing algorithm, random forest, and shows that almost all LLMs exhibit no trace of significant differences between the forecasted and observed math scores in the years before the pandemic (only 2% of the LLMs report a difference lower than -1 standard deviation).²⁶

Finally, Figure 3 reports a diagnostic test for the performance of the MLCM with random forest. The figure illustrates that the distribution of the placebo forecasting errors is approximately normal and centered around zero, not only for the temporal average but also for the single pre-treatment years. This demonstrates that the ATE estimator is nearly unbiased even when applied on very short panels and without relying on post-treatment information.

²⁶Figure 6 in Appendix E presents the placebo maps for the single pre-treatment years (2018 and 2019). In this instance as well, very few LLMs exhibit a difference lower than -1 standard deviation between the forecasted and observed math scores prior to the pandemic (4.3% of LLMs in 2018 and 5.7% of LLMs in 2019). Furthermore, the LLMs with extreme values tend to be the smallest ones, which are also the most volatile.

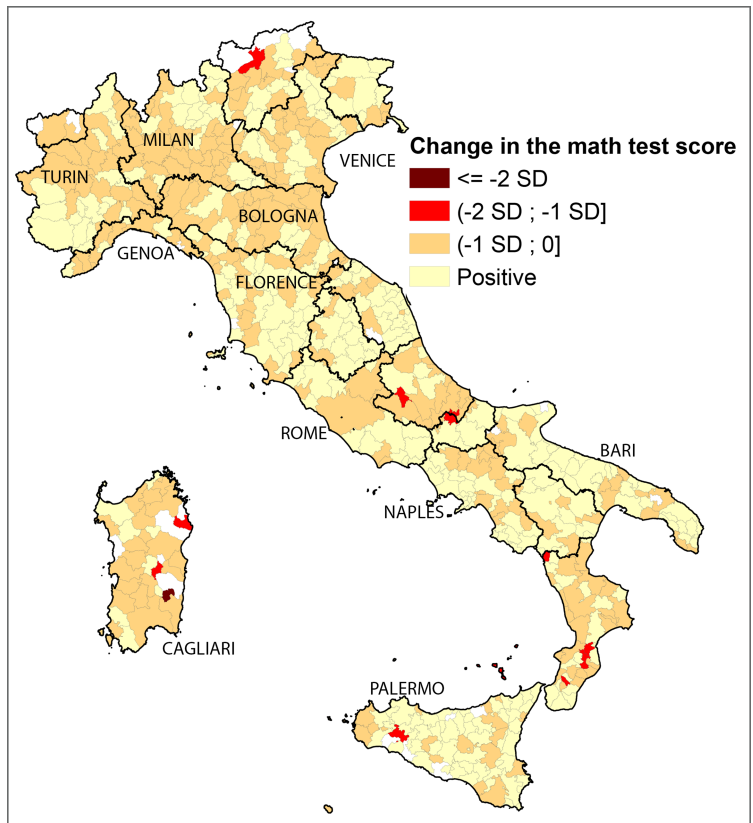


Figure 2: Unit-level panel placebo test—Temporal average ‘treatment’ effects. Note: the standard deviation (SD) refers to the standardized pre-COVID mean. Estimation via the MLCM with random forest.

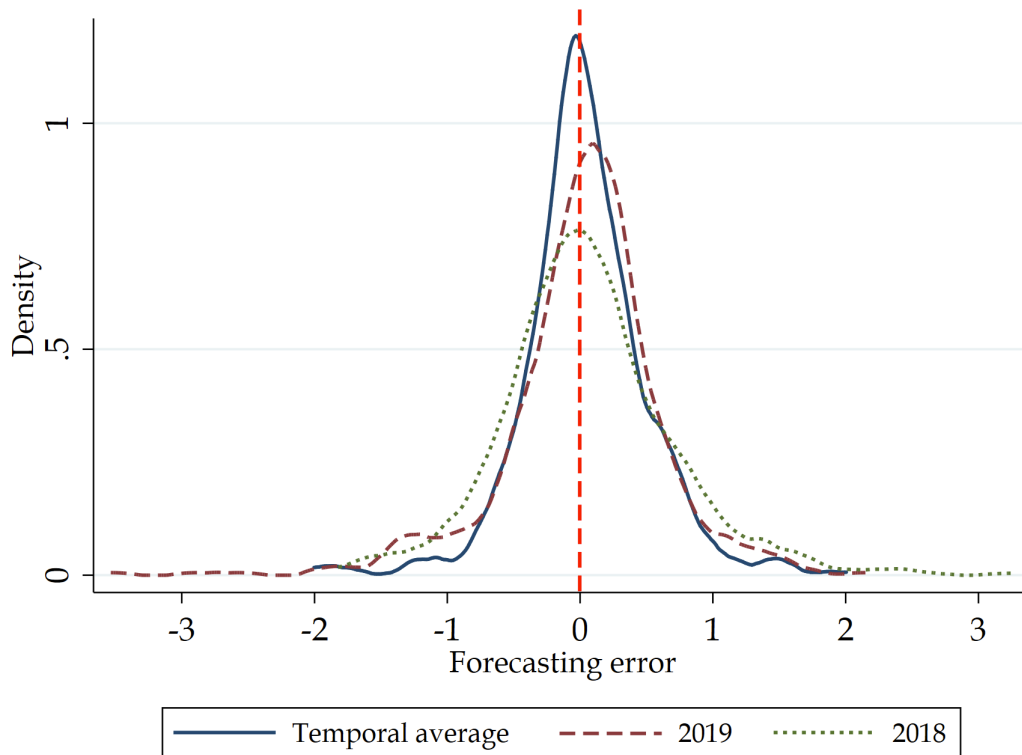


Figure 3: Distribution of the forecasting error. Note: Forecasting errors of the MLCM estimated with random forest.

4.3.2 Analysis Stage

Figure 4 shows the local effects of the pandemic on math scores of fifth-grade students across Italian LLMs and reports the ATE. These estimates come from the best-performing technique of the Design stage, the MLCM with random forest.

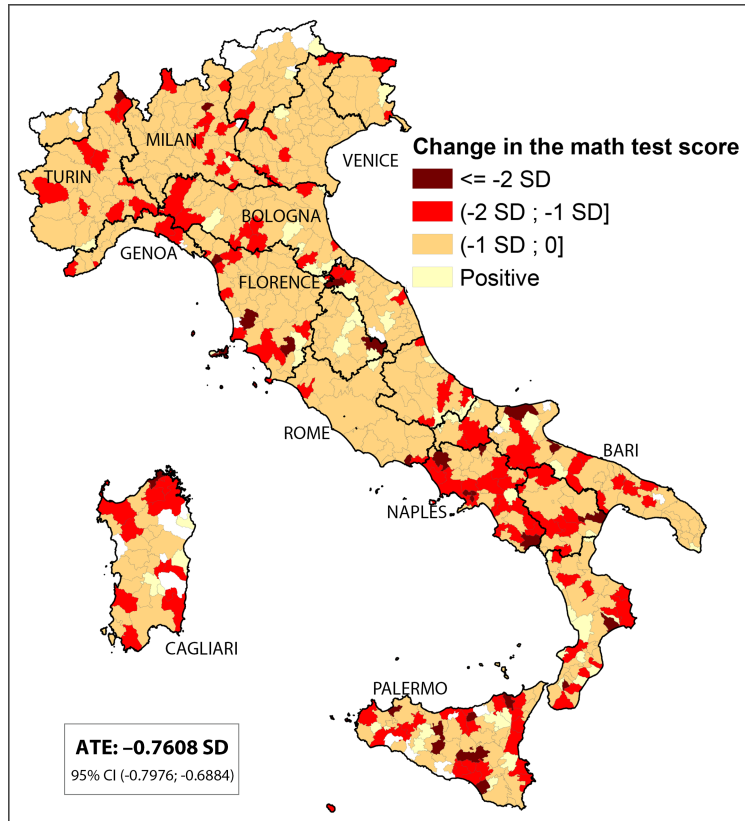


Figure 4: The local impact of the COVID-19 pandemic on education.

The first main insight is that the COVID-19 shock engendered major learning losses in Italy. The ATE points to a decrease in the math score of -0.7608 standard deviation (SD) with respect to the pre-pandemic average, and this effect is strongly statistically significant with 95% confidence intervals (-0.7976 ; -0.6884). This result is in line with new micro-level studies documenting large negative impacts on educational outcomes in Italy (Battisti and Maggio, 2023; Carlana et al., 2023).

As shown above, some of the smallest LLMs (the most volatile) were imprecisely estimated in the placebo exercise. Consequently, since equal weight is attributed to all treated units, the presence of these LLMs might affect the accuracy of the ATE estimate. In general, to address this potential concern, we recommend a sensitivity analysis that re-estimates the ATE following the exclusion of units with the poorest fit in the pre-treatment period. In our application, we removed the top 1%, 2%, and 5% of the most imprecisely estimated LLMs in the placebo tests. The resultant ATE estimates were -0.7500 , -0.7568 , and -0.7341 , respectively—each closely aligning with the ATE estimate of -0.7608 .²⁷

The second key finding is that this average impact masks considerable heterogeneity across the Italian territory. Some LLMs experienced drops in students' performances much larger than the ATE. In particular, the MLCM detects learning losses of more than one standard deviation in clusters of local economies mostly, but not exclusively, located in the South of Italy (Campania, Apulia, Molise,

²⁷This sensitivity test mirrors the approach proposed by Abadie et al. (2010) for the synthetic control method, which involves removing the untreated units that were imprecisely estimated from the in-space placebo test.

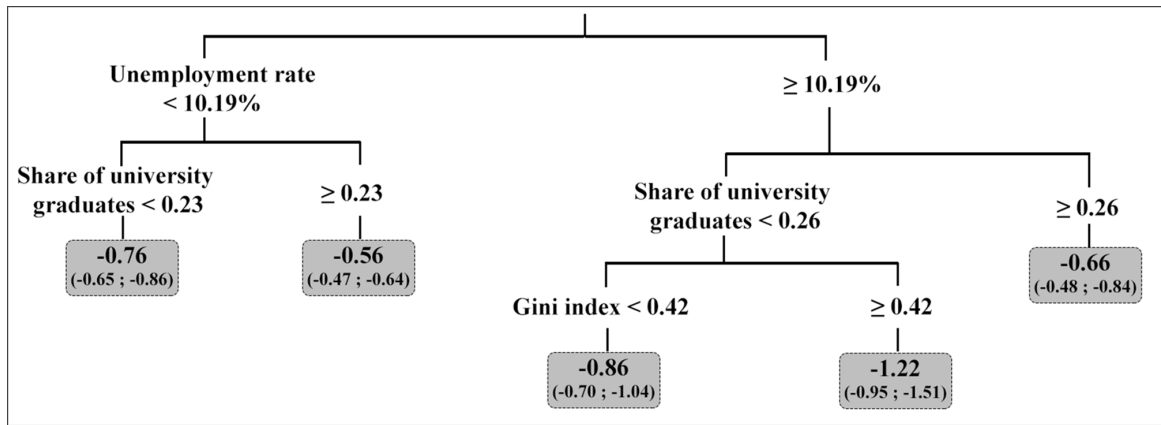


Figure 5: Data-driven CATEs. Note: The values within the terminal nodes report the CATEs (measured in SD) for all LLMs grouped within that node. Lower and upper bounds refer to the 95% confidence interval and are reported in parentheses.

Calabria, Sicily, and Sardinia), and drops in math scores greater than two SD in scattered areas predominantly concentrated in Central and Southern regions.

Figure 5 presents data-driven CATEs estimated with the regression tree analysis.²⁸ The algorithm selects only three predictors to construct the tree. The analysis reveals that the most substantial learning losses (1.22 SD below the pre-COVID baseline) occurred in LLMs characterized by an unemployment rate equal to or above 10.19%, a percentage of university graduates below 26%, and a Gini index equal to or above 0.42. Conversely, the territories with an above-average treatment effect (−0.56 SD) exhibit an unemployment rate below 10.19% and a percentage of university graduates equal to or above 23%. Finally, all the CATEs reported in the tree are statistically significant.

Given that areas with higher unemployment, greater inequality, and lower education rates at baseline have experienced disproportionate impacts, the pre-existing gaps across the country have been amplified. If such gaps persist, it is likely that these educational inequalities will, in turn, act as a catalyst for future economic inequality, leading to widened territorial disparities in the medium and long term. In summary, we can reasonably anticipate that, in the absence of counterbalancing policy efforts, the pandemic will exacerbate long-standing inequalities that predate COVID-19.

5 Conclusions

We propose a new causal panel data method based on flexible counterfactual forecasting with machine learning. The MLCM can employ any off-the-shelf ML technique and enables the estimation of policy-relevant causal parameters in evaluation settings with short and long panels and without a control group. The method is embedded within the potential outcomes framework and based on panel CV for estimation and bootstrap methods to conduct inference. To illustrate the potential of the MLCM, we presented numerical studies and an empirical analysis on the effects of the COVID-19 crisis on education in Italy, which revealed a generalized drop in students’ performance and significant inequalities in learning losses across the Italian territory. The companion R package `MachineControl`

²⁸For this analysis, we selected, on the basis of domain knowledge, a set of LLM-level variables potentially associated with the estimated treatment effects, including, among others, pre-pandemic variables such as the per capita income, the unemployment rate, the Gini index, the share of university graduates, and two proxies of access to distance learning that capture the digital divide across areas. We also included excess deaths registered during the first wave of the pandemic (Cerqua et al., 2021). The full list of predictors included in the regression tree CATE model can be found in Table 14 in Appendix E.

provides an easy-to-use implementation of the proposed approach. Large-scale shocks, international economic policies, nationwide policy changes, regional programs and local interventions engendering substantial interaction between units, are all real-world scenarios in which a suitable control group may not exist. In such cases, researchers can harness the MLCM, which complements the existing econometric toolbox for causal inference and program evaluation.

References

- Abadie, A. (2021). Using synthetic controls: Feasibility, data requirements, and methodological aspects. *Journal of Economic Literature*, 59(2):391–425. [12](#)
- Abadie, A., Diamond, A., and Hainmueller, J. (2010). Synthetic control methods for comparative case studies: Estimating the effect of California’s tobacco control program. *Journal of the American Statistical Association*, 105(490):493–505. [2](#), [5](#), [24](#)
- Agostinelli, F., Doepke, M., Sorrenti, G., and Zilibotti, F. (2022). When the great equalizer shuts down: Schools, peers, and parents in pandemic times. *Journal of Public Economics*, 206:104574. [18](#)
- Angrist, J. D. and Pischke, J.-S. (2009). *Mostly harmless econometrics: An empiricist’s companion*. Princeton university press. [2](#)
- Arkhangelsky, D., Athey, S., Hirshberg, D. A., Imbens, G. W., and Wager, S. (2021). Synthetic difference-in-differences. *American Economic Review*, 111(12):4088–4118. [2](#)
- Arkhangelsky, D. and Imbens, G. (2023). Causal models for longitudinal and panel data: A survey. *arXiv preprint arXiv:2311.15458*. [12](#)
- Ashenfelter, O. and Card, D. (1985). Using the longitudinal structure of earnings to estimate the effect of training programs. *The Review of Economics and Statistics*, 67(4):648–660. [2](#)
- Athey, S., Bayati, M., Doudchenko, N., Imbens, G., and Khosravi, K. (2021). Matrix completion methods for causal panel data models. *Journal of the American Statistical Association*, 116(536):1716–1730. [2](#)
- Athey, S. and Imbens, G. (2016). Recursive partitioning for heterogeneous causal effects. *Proceedings of the National Academy of Sciences*, 113(27):7353–7360. [3](#), [16](#)
- Athey, S., Simon, L. K., Skans, O. N., Vikstrom, J., and Yakymovych, Y. (2023). The heterogeneous earnings impact of job loss across workers, establishments, and markets. *arXiv preprint arXiv:2307.06684*. [3](#)
- Athey, S. and Wager, S. (2019). Estimating treatment effects with causal forests: An application. *Observational Studies*, 5(2):37–51. [19](#)
- Bai, J. (2009). Panel data models with interactive fixed effects. *Econometrica*, 77(4):1229–1279. [2](#)
- Baltagi, B. H. (2008). *Econometric analysis of panel data*, volume 4. Springer. [9](#), [10](#)
- Basu, S., Kumbier, K., Brown, J. B., and Yu, B. (2018). Iterative random forests to discover predictive and stable high-order interactions. *Proceedings of the National Academy of Sciences*, 115(8):1943–1948. [19](#)
- Battisti, M. and Maggio, G. (2023). Will the last be the first? School closures and educational outcomes. *European Economic Review*, 154:104405. [18](#), [19](#), [24](#)
- Bertrand, M., Duflo, E., and Mullainathan, S. (2004). How much should we trust differences-in-differences estimates? *The Quarterly Journal of Economics*, 119(1):249–275. [21](#)

- Borusyak, K., Jaravel, X., and Spiess, J. (2023). Revisiting event study designs: Robust and efficient estimation. *Review of Economic Studies*, forthcoming. 5
- Botosaru, I., Giacomini, R., and Weidner, M. (2023). Forecasted treatment effects. *arXiv preprint*. Available at <https://arxiv.org/abs/2309.05639>. 3
- Box, G. E. and Tiao, G. C. (1975). Intervention analysis with applications to economic and environmental problems. *Journal of the American Statistical Association*, 70(349):70–79. 3
- Britto, D. G., Pinotti, P., and Sampaio, B. (2022). The effect of job loss and unemployment insurance on crime in brazil. *Econometrica*, 90(4):1393–1423. 3
- Brodersen, K. H., Gallusser, F., Koehler, J., Remy, N., and Scott, S. L. (2015). Inferring causal impact using bayesian structural time-series models. *The Annals of Applied Statistics*, 9(1):247. 3, 6
- Card, D. (1990). The impact of the Mariel boatlift on the Miami labor market. *Industrial and Labor Relations Review*, 43(2):245–257. 2
- Card, D. and Krueger, A. B. (1994). Minimum wages and employment: A case study of the fast-food industry in New Jersey and Pennsylvania. *The American Economic Review*, 84(4):772–793. 2
- Carlana, M., La Ferrara, E., and Lopez, C. (2023). Exacerbated inequalities: The learning loss from covid-19 in italy. *AEA Papers and Proceedings*, 113:489–93. 18, 19, 24, 42
- Carlstein, E. (1986). The use of subseries values for estimating the variance of a general statistic from a stationary sequence. *The Annals of Statistics*, 14(3):1171–1179. 31
- Carvalho, C., Masini, R., and Medeiros, M. C. (2018). ArCo: An artificial counterfactual approach for high-dimensional panel time-series data. *Journal of econometrics*, 207(2):352–380. 3, 9
- Cerqua, A., Di Stefano, R., Letta, M., and Miccoli, S. (2021). Local mortality estimates during the covid-19 pandemic in italy. *Journal of Population Economics*, 34(4):1189–1217. 25, 45
- Chernozhukov, V., Demirer, M., Duflo, E., and Fernandez-Val, I. (2018). Generic machine learning inference on heterogeneous treatment effects in randomized experiments, with an application to immunization in India. Technical report, National Bureau of Economic Research. 7
- Chernozhukov, V., Wüthrich, K., and Zhu, Y. (2021). An exact and robust conformal inference method for counterfactual and synthetic controls. *Journal of the American Statistical Association*, 116(536):1849–1864. 3
- Chiu, A., Lan, X., Liu, Z., and Xu, Y. (2023). What to do (and not to do) with causal panel analysis under parallel trends: Lessons from a large reanalysis study. *arXiv preprint*. Available at [arXiv:2309.15983](https://arxiv.org/abs/2309.15983). 5
- Cox, D. R. (1958). *Planning of experiments*. Wiley, New York, NY. 2, 5
- D’Haultfoeuille, X., Hoderlein, S., and Sasaki, Y. (2023). Nonparametric difference-in-differences in repeated cross-sections with continuous treatments. *Journal of Econometrics*, 234(2):664–690. 6
- Duflo, E. (2017). The economist as plumber. *American Economic Review*, 107(5):1–26. 2

- Eggers, A. C., Tuñón, G., and Dafoe, A. (2021). Placebo tests for causal inference. *American Journal of Political Science*. Forthcoming. [14](#)
- Fan, Q., Hsu, Y.-C., Lieli, R. P., and Zhang, Y. (2022). Estimation of conditional average treatment effects with high-dimensional data. *Journal of Business & Economic Statistics*, 40(1):313–327. [7](#)
- Friedman, J. H. (2001). Greedy function approximation: A gradient boosting machine. *The Annals of Statistics*, 29(5):1189–1232. [34](#)
- Friedman, J. H. (2002). Stochastic gradient boosting. *Computational Statistics & Data Analysis*, 38(4):367–378. [34](#)
- Geladi, P. and Kowalski, B. R. (1986). Partial least-squares regression: a tutorial. *Analytica chimica acta*, 185:1–17. [33](#)
- Hoderlein, S. and White, H. (2012). Nonparametric identification in nonseparable panel data models with generalized fixed effects. *Journal of Econometrics*, 168(2):300–314. [6](#)
- Holland, P. W. (1986). Statistics and causal inference. *Journal of the American statistical Association*, 81(396):945–960. [2](#)
- Hyndman, R. J. and Athanasopoulos, G. (2021). *Forecasting: principles and practice*. OTexts, Melbourne, Australia. [3](#), [14](#)
- Imbens, G. W. and Rubin, D. B. (2015). *Causal inference in Statistics, Social, and Biomedical Sciences*. Cambridge University Press, Cambridge, UK. [2](#), [5](#), [7](#)
- Johannemann, J., Hadad, V., Athey, S., and Wager, S. (2019). Sufficient representations for categorical variables. arXiv preprint. Available at [arXiv:1908.09874](#). [10](#)
- Knaus, M. C., Lechner, M., and Strittmatter, A. (2021). Machine learning estimation of heterogeneous causal effects: Empirical Monte Carlo evidence. *The Econometrics Journal*, 24(1):134–161. [7](#)
- Kuhn, M. and Johnson, K. (2013). *Applied predictive modeling*, volume 26. Springer, New York, NY. [13](#), [14](#)
- Kunsch, H. R. (1989). The jackknife and the bootstrap for general stationary observations. *The Annals of Statistics*, 17(3):1217–1241. [31](#)
- Liu, L., Wang, Y., and Xu, Y. (2022). A practical guide to counterfactual estimators for causal inference with time-series cross-sectional data. *American Journal of Political Science*. [14](#), [21](#)
- Masini, R. and Medeiros, M. C. (2021). Counterfactual analysis with artificial controls: Inference, high dimensions, and nonstationarity. *Journal of the American Statistical Association*, 116(536):1773–1788. [3](#), [7](#), [9](#)
- Menchetti, F., Cipollini, F., and Mealli, F. (2023). Combining counterfactual outcomes and arima models for policy evaluation. *The Econometrics Journal*, 26(1):1–24. [3](#)
- Mullainathan, S. and Spiess, J. (2017). Machine learning: an applied econometric approach. *Journal of Economic Perspectives*, 31(2):87–106. [12](#)

- Ogburn, E. L. and VanderWeele, T. J. (2014). Causal diagrams for interference. *Statistical Science*, 29(4):559–578. 5
- Rambachan, A. and Roth, J. (2023). A more credible approach to parallel trends. *The Review of Economic Studies*, 90:2555–2591. 7
- Roth, J., Sant’Anna, P. H., Bilinski, A., and Poe, J. (2023). What’s trending in difference-in-differences? a synthesis of the recent econometrics literature. *Journal of Econometrics*, 235:2218–2244. 2
- Rubin, D. B. (1974). Estimating causal effects of treatments in randomized and nonrandomized studies. *Journal of Educational Psychology*, 66(5):688–701. 2, 5
- Sobel, M. E. (2006). What do randomized studies of housing mobility demonstrate? causal inference in the face of interference. *Journal of the American Statistical Association*, 101(476):1398–1407. 2, 5
- Stantcheva, S. (2022). Inequalities in the times of a pandemic. *Economic Policy*, 37(109):5–41. 18, 19
- Tibshirani, R. (1996). Regression shrinkage and selection via the Lasso. *Journal of the Royal Statistical Society Series B: Statistical Methodology*, 58(1):267–288. 33
- Varian, H. R. (2016). Causal inference in economics and marketing. *Proceedings of the National Academy of Sciences*, 113(27):7310–7315. 3
- Verbeek, M. (2017). *A guide to modern econometrics*. John Wiley & Sons. 10
- Viviano, D. and Bradic, J. (2023). Synthetic learner: model-free inference on treatments over time. *Journal of Econometrics*, 234(2):691–713. 3, 9, 31
- Wager, S. and Athey, S. (2018). Estimation and inference of heterogeneous treatment effects using random forests. *Journal of the American Statistical Association*, 113(523):1228–1242. 3, 9, 16
- Werner, K. and Woessmann, L. (2023). The legacy of COVID-19 in education. *Economic Policy*, page eiad016. 18
- Xu, Y. (2023). Causal inference with time-series cross-sectional data: a reflection. *The Oxford Handbook for Methodological Pluralism*. Forthcoming. 5

Appendices

A Bootstrap inference for ATE and CATE confidence intervals

Following recent work on causal machine learning estimators for panel data (Viviano and Bradic, 2023), inference on causal effects estimated with the MLCM is performed by block-bootstrap. Since we are dealing with a panel dataset that has an inherent temporal structure, resampling the unit-time pairs independently in a context with dependent data would lead to data leakage. Therefore, we sample the units instead of the unit-time pairs so that if a unit is sampled, its entire evolution over time is sampled as well. This way, the inference is more robust to misspecification issues. This idea is in the spirit of the original block-bootstrap introduced by Carlstein (1986) and Kunsch (1989) that consists in dividing a time series in blocks (overlapping or non-overlapping) and then sampling the blocks with replacement. Since we have a panel dataset, we can consider each unit to form one block. The full algorithm to derive block-bootstrap confidence intervals in our setting is detailed in Algorithm 1 below.

Algorithm 1 Block-bootstrap algorithm for ATE

Require: N, B ,

- 1: **for** b in $1 : B$ where B is the total number of bootstrap iterations **do**
 - 2: Sample N units with replacement
 - 3: Only for the resampled units, retain the tuple $(Y_{i,t}^*, \mathcal{Y}_{i,t-1}^{(p)*}(0), \mathbf{X}_{i,t}^*, \mathcal{X}_{i,t-1}^{(q)*})^{(b)}$ for all $t = 1, \dots, T$ (pre- and post-intervention)
 - 4: Compute the bootstrap replication of the ATE, i.e., $\hat{\tau}_t^*(b)$ by repeating the Design stage (steps 3 to 5) and the Analysis stage (steps 6 to 9) of the MLCM outlined in Section 3
 - 5: **end for**
 - 6: Let $\hat{G}(c) = \#\{\hat{\tau}_t^*(b) \leq c\}/B$ be the empirical cumulative distribution function of the B bootstrap replications. Compute a $(1 - \alpha)$ percentile interval as $[\hat{G}^{-1}(\alpha/2), \hat{G}^{-1}(1 - \alpha/2)]$.
-

Deriving confidence intervals for the CATEs is more challenging than for the ATE. The reason is that CATEs are estimated with a regression tree where the outcome is a collection of individual causal effects. Therefore, if we resample the units at the very beginning and then we estimate B different CATEs, we will end up with very different trees: both the splits and the observations within each terminal node will likely differ. For this reason, we propose to resample directly the observations within each terminal node of the tree. Note that the observations are the estimated individual causal effects (computed by comparing the observed data with the ML forecasts). Our estimand of interest is the group-average of the individual effects, so at each bootstrap iteration, we resample the units in each terminal node, averaging the individual effects and obtaining a bootstrap distribution for the CATE. The full algorithm to derive confidence intervals is described in Algorithm 2 below.

Algorithm 2 Block-bootstrap algorithm for CATEs

Require: $\hat{\tau}_t, \mathbf{X}_{i,t}, D, B,$

- 1: **for** b in $1 : B$ where B is the total number of bootstrap iterations and for $d = 1, \dots, D$ where D is the total number of terminal nodes of the tree **do**
 - 2: Sample with replacement the N_d units in terminal node d
 - 3: Only for the resampled units, retain the tuple $(\hat{\tau}_t^*, \mathbf{X}_{i,t}^*)_d^{(b)}$
 - 4: Compute the bootstrap replication of CATE in the terminal node d by averaging the ATEs of the resampled units, i.e., $\hat{\tau}_t^*(d)$.
 - 5: By definition (6), $\hat{\tau}_t^*(d)$ is an estimator of CATE, since we are averaging the individual effects among the units in group (terminal node) d , i.e., we are conditioning on covariates
 - 6: **end for**
 - 7: Let $\hat{G}(c) = \#\{\hat{\tau}_t^*(d) \leq c\}/B$ be the empirical cumulative distribution function of the d -group CATE in the B bootstrap replication. Compute a $(1 - \alpha)$ percentile interval as $[\hat{G}^{-1}(\alpha/2), \hat{G}^{-1}(1 - \alpha/2)]$.
-

B Overview of the ML models employed in the application

This appendix provides an overview of the ML algorithms employed in both the simulation study of section 3.3 and the empirical application of section 4. We remark that modeling potential outcomes in the absence of the treatment according to Equation (2) reflects our uncertainty on $Y_{i,t}(0)$ rather than an assumption on the distribution of potential outcomes in the superpopulation, as we already observe the entire population under study. As discussed in the main text, we tested several ML methods to learn the function $f(\cdot)$. Thus, we provide some examples of what the causal effect estimators look like for some of the supervised ML methods that can be employed by the MLCM. Specifically, we show the cases of the four ML algorithms employed in the empirical application.

- LASSO

Assuming a linear functional form for $f(\cdot)$ in Equation (2), an estimator for the unobserved potential outcome in the absence of the intervention can be written as,

$$\begin{aligned} Y_{i,t_0+k|t_0}(0) &= \mathbb{E}[Y_{i,t_0+k}(0)|\mathcal{I}_{t_0}, \mathbf{X}_{i,t_0+k}] \\ &= \mathbb{E} \left[\sum_{j=1}^p \hat{\phi}_j Y_{i,t_0+k-j}(0)|\mathcal{I}_{t_0}, \mathbf{X}_{i,t_0+k} \right] + \sum_{j=0}^q \mathbf{X}_{i,t_0+k-j} \hat{\boldsymbol{\beta}}. \end{aligned}$$

This can be recursively computed from $Y_{i,t_0+1|t_0}(0)$ as follows:

$$\begin{aligned} Y_{i,t_0+1|t_0}(0) &= \mathbb{E}[Y_{i,t_0+1}(0)|\mathcal{I}_{t_0}, \mathbf{X}_{i,t_0+1}] \\ &= \sum_{j=1}^p \hat{\phi}_j Y_{i,t_0+1-j} + \sum_{j=0}^q \mathbf{X}_{i,t_0-j+1} \hat{\boldsymbol{\beta}} \\ Y_{i,t_0+2|t_0}(0) &= \phi_1 \mathbb{E}[Y_{i,t_0+1}(0)|\mathcal{I}_{t_0}, \mathbf{X}_{i,t_0+2}] + \sum_{j=2}^p \hat{\phi}_j Y_{i,t_0+2-j} + \sum_{j=0}^q \mathbf{X}_{i,t_0-j+2} \hat{\boldsymbol{\beta}} \end{aligned}$$

where $(\hat{\phi}_1, \dots, \hat{\phi}_p, \hat{\boldsymbol{\beta}})$ are estimated as in Tibshirani (1996) by minimizing a penalized version of the residual sum of squares.

- Partial Least Squares

$$\begin{aligned} Y_{i,t_0+k|t_0}(0) &= \mathbb{E}[Y_{i,t_0+k}(0)|\mathcal{I}_{t_0}, \mathbf{X}_{i,t_0+k}] \\ &= \mathbb{E} \left[\sum_{j=1}^p \hat{\phi}_j Y_{i,t_0+k-j}(0)|\mathcal{I}_{t_0}, \mathbf{X}_{i,t_0+k} \right] + \sum_{j=0}^q \mathbf{X}_{i,t_0+k-j} \hat{\boldsymbol{\beta}}^{\text{PLS}} \\ &= \sum_{j=1}^p \hat{\phi}_j^{\text{PLS}} Y_{i,t_0+1-j} + \sum_{j=0}^q \mathbf{X}_{i,t_0-j+1} \hat{\boldsymbol{\beta}}^{\text{PLS}} \end{aligned}$$

where $(\hat{\phi}_1^{\text{PLS}}, \dots, \hat{\phi}_p^{\text{PLS}}, \hat{\boldsymbol{\beta}}^{\text{PLS}})$ are estimated as in Geladi and Kowalski (1986).

- Stochastic Gradient Boosting

$$\begin{aligned} Y_{i,t_0+k|t_0}(0) &= \mathbb{E}[Y_{i,t_0+k}(0)|\mathcal{I}_{t_0}, \mathbf{X}_{i,t_0+k}] \\ &= \sum_{s=1}^S \beta_s h_s \left(\mathcal{Y}_{i,t_0+k-1}^{(p)}(0), \mathbf{X}_{i,t_0+k}, \mathcal{X}_{i,t_0+k-1}^{(q)} \right) \end{aligned}$$

where, following [Friedman \(2001\)](#), h_s are the so-called “base” learners chosen to be simple functions of the covariates over S samples. We employ stochastic gradient boosting instead of conventional gradient boosting due to its enhanced approximation accuracy and faster execution speed ([Friedman, 2002](#)).

- Random Forest

$$\begin{aligned} Y_{i,t_0+k|t_0}(0) &= \mathbb{E}[Y_{i,t_0+k}(0)|\mathcal{I}_{t_0}, \mathbf{X}_{i,t_0+k}] \\ &= \frac{1}{A} \sum_{a=1}^A T^{(a)} \left(\mathcal{Y}_{i,t_0+k-1}^{(p)}(0), \mathbf{X}_{i,t_0+k}, \mathcal{X}_{i,t_0+k-1}^{(q)}; R_Y, \mu \right). \end{aligned}$$

In the latter equation, $T(\cdot)$ denotes a single tree, defined as,

$$T \left(\mathcal{Y}_{i,t_0+k-1}^{(p)}(0), \mathbf{X}_{i,t_0+k}, \mathcal{X}_{i,t_0+k-1}^{(q)}; R_Y, \mu \right) = \sum_{l=1}^L \mu_l \mathbb{I}_{\{(\mathcal{Y}, \mathbf{X}, \mathcal{X})_{t_0+k} \in R_l\}}$$

where R_Y is a binary recursive partition of the covariates space, l is the number of leaf nodes, μ_l are the parameters and $\mathbb{I}_{\{(\mathcal{Y}, \mathbf{X}, \mathcal{X})_{t_0+k} \in R_l\}}$ is an indicator function taking value 1 when unit i (as defined by its covariate set) at time $t_0 + k$ falls in the partition R_l . Finally, A is the number of trees forming the forest.

C Causal estimands in settings with interference between units

Compared to Case (i), in the scenario with violations of the no-interference assumption, the causal estimands are different. In this section, we define causal estimands for the setup in which only a subgroup of units gets treated, but there are likely spillover and general equilibrium effects that prevent using the set of untreated units to build a valid control group (Case (ii) defined above). We can first define the ATT across the treated units at a given point in time.

Definition 6 For any strictly positive integer k , let $\tau_{i,t_0+k} = Y_{i,t_0+k}(1) - Y_{i,t_0+k|t_0}(0)$ be the unit-level treatment effect of the policy at time $t_0 + k$ and denote with N_T the number of treated units. The ATT at time $t_0 + k$ is defined as,

$$\tau_{t_0+k}^T = \frac{1}{N_T} \sum_{i=1}^{N_T} \tau_{i,t_0+k} = \frac{1}{N_T} \sum_{i=1}^{N_T} Y_{i,t_0+k}(1) - Y_{i,t_0+k|t_0}(0).$$

Note that, in this framework, the ATE does not coincide with the ATT because not all units are directly exposed to the treatment.

As a subgroup of the units is not treated but potentially subject to spillovers, we can define the Average Spillover effect on the Affected (ASA) across the untreated units at a given point in time.

Definition 7 For any strictly positive integer k , let $\tau_{j,t_0+k} = Y_{j,t_0+k}(1) - Y_{j,t_0+k|t_0}(0)$ denote the unit-level spillover effect of the policy at time $t_0 + k$ for all untreated units and denote with N_C the number of untreated units. The ASA at time $t_0 + k$ is defined as,

$$\tau_{t_0+k}^C = \frac{1}{N_C} \sum_{j=1}^{N_C} \tau_{j,t_0+k} = \frac{1}{N_C} \sum_{j=1}^{N_C} Y_{j,t_0+k}(1) - Y_{j,t_0+k|t_0}(0).$$

Both causal estimands, $\tau_{t_0+k}^T$ and $\tau_{t_0+k}^C$, can be estimated with the MLCM by applying the same implementation routine defined in the paper separately for the group of treated and untreated units.

D Additional simulation results

In this Section of the Appendix we report the results of all the simulation scenarios that we generated by combining the following parameters: i) number of units in the panel ($N = 400, N = 200$); ii) autoregressive coefficient ($\phi = 0.8, \phi = 1.2$); iii) standard deviation of u_i regulating the amount of heterogeneity between units ($\sigma_u = 1, \sigma_u = 0.1$).

Table 4 shows the results of an “explosive” simulation scenario corresponding to the one reported in the main text ($N = 400, \sigma_u = 1$), but with $\phi = 1.2$. Tables 5 and 6 report the results for the remaining combinations with $N = 400$ and $\sigma_u = 0.1$.

Tables 7–10 show the results of the simulations when the number of units in the panel reduces to $N = 200$.

Table 4: Simulation results for $N = 400, \phi = 1.2$ and $\sigma_u = 1$

		1st Post-intervention period ($t_0 + 1$)							
		Linear				Non-Linear			
Pre-int.	Bootstrap	True ATE	Bias	Rel. Bias	Coverage	True ATE	Bias	Rel. Bias	Coverage
4	block	234.28	0.17	0.001	0.94	4.07	0.10	0.024	0.95
9	block	641.62	0.12	0.000	0.94	4.14	0.09	0.023	0.95
		2nd Post-intervention period ($t_0 + 2$)							
		Linear				Non-Linear			
Pre-int.	Bootstrap	True ATE	Bias	Rel. Bias	Coverage	True ATE	Bias	Rel. Bias	Coverage
4	block	175.71	0.39	0.002	0.93	3.05	0.10	0.032	0.91
9	block	481.21	0.25	0.001	0.92	3.10	0.10	0.031	0.92
		3rd Post-intervention period ($t_0 + 3$)							
		Linear				Non-Linear			
Pre-int.	Bootstrap	True ATE	Bias	Rel. Bias	Coverage	True ATE	Bias	Rel. Bias	Coverage
4	block	117.14	0.75	0.006	0.93	2.03	0.10	0.050	0.92
9	block	320.81	0.46	0.001	0.94	2.07	0.09	0.045	0.92

Table 5: Simulation results for $N = 400, \phi = 0.8$ and $\sigma_u = 0.1$

		1st Post-intervention period ($t_0 + 1$)							
		Linear				Non-Linear			
Pre-int.	Bootstrap	True ATE	Bias	Rel. Bias	Coverage	True ATE	Bias	Rel. Bias	Coverage
4	block	73.38	0.27	0.004	0.97	4.07	0.14	0.033	0.97
9	block	92.58	0.15	0.002	0.95	4.14	0.11	0.027	0.95
		2nd Post-intervention period ($t_0 + 2$)							
		Linear				Non-Linear			
Pre-int.	Bootstrap	True ATE	Bias	Rel. Bias	Coverage	True ATE	Bias	Rel. Bias	Coverage
4	block	55.03	0.37	0.007	0.94	3.05	0.10	0.034	0.91
9	block	69.44	0.21	0.003	0.93	3.10	0.11	0.034	0.93
		3rd Post-intervention period ($t_0 + 3$)							
		Linear				Non-Linear			
Pre-int.	Bootstrap	True ATE	Bias	Rel. Bias	Coverage	True ATE	Bias	Rel. Bias	Coverage
4	block	36.69	0.72	0.020	0.94	2.04	0.14	0.071	0.95
9	block	46.29	0.33	0.007	0.94	2.07	0.11	0.051	0.93

Table 6: Simulation results for $N = 400$, $\phi = 1.2$ and $\sigma_u = 0.1$

		1st Post-intervention period ($t_0 + 1$)							
		Linear				Non-Linear			
Pre-int.	Bootstrap	True ATE	Bias	Rel. Bias	Coverage	True ATE	Bias	Rel. Bias	Coverage
4	block	233.97	0.31	0.001	0.96	4.07	0.14	0.034	0.97
9	block	640.02	0.18	0.000	0.95	4.14	0.11	0.027	0.95
		2nd Post-intervention period ($t_0 + 2$)							
		Linear				Non-Linear			
Pre-int.	Bootstrap	True ATE	Bias	Rel. Bias	Coverage	True ATE	Bias	Rel. Bias	Coverage
4	block	175.47	0.65	0.004	0.95	3.05	0.10	0.034	0.92
9	block	480.01	0.36	0.001	0.94	3.11	0.11	0.034	0.94
		3rd Post-intervention period ($t_0 + 3$)							
		Linear				Non-Linear			
Pre-int.	Bootstrap	True ATE	Bias	Rel. Bias	Coverage	True ATE	Bias	Rel. Bias	Coverage
4	block	116.98	1.34	0.011	0.95	2.03	0.15	0.073	0.95
9	block	320.01	0.72	0.002	0.95	2.07	0.10	0.051	0.94

Table 7: Simulation results for $N = 200$ units, $\phi = 0.8$ and $\sigma_u = 1$

		1st Post-intervention period ($t_0 + 1$)							
		Linear				Non-Linear			
Pre-int.	Bootstrap	True ATE	Bias	Rel. Bias	Coverage	True ATE	Bias	Rel. Bias	Coverage
4	block	74.23	0.22	0.003	0.93	4.07	0.13	0.033	0.97
9	block	92.07	0.15	0.002	0.94	4.14	0.13	0.032	0.94
		2nd Post-intervention period ($t_0 + 2$)							
		Linear				Non-Linear			
Pre-int.	Bootstrap	True ATE	Bias	Rel. Bias	Coverage	True ATE	Bias	Rel. Bias	Coverage
4	block	55.67	0.36	0.006	0.90	3.05	0.13	0.044	0.92
9	block	69.06	0.22	0.003	0.90	3.11	0.13	0.042	0.93
		3rd Post-intervention period ($t_0 + 3$)							
		Linear				Non-Linear			
Pre-int.	Bootstrap	True ATE	Bias	Rel. Bias	Coverage	True ATE	Bias	Rel. Bias	Coverage
4	block	37.11	0.48	0.013	0.93	2.04	0.14	0.068	0.93
9	block	46.04	0.29	0.006	0.92	2.07	0.13	0.064	0.92

Table 8: Simulation results for $N = 200$ units, $\phi = 0.8$ and $\sigma_u = 0.1$

		1st Post-intervention period ($t_0 + 1$)							
		Linear				Non-Linear			
Pre-int.	Bootstrap	True ATE	Bias	Rel. Bias	Coverage	True ATE	Bias	Rel. Bias	Coverage
4	block	73.34	0.41	0.006	0.96	4.07	0.19	0.046	0.96
9	block	91.86	0.21	0.002	0.94	4.14	0.15	0.037	0.95
		2nd Post-intervention period ($t_0 + 2$)							
		Linear				Non-Linear			
Pre-int.	Bootstrap	True ATE	Bias	Rel. Bias	Coverage	True ATE	Bias	Rel. Bias	Coverage
4	block	55.01	0.56	0.010	0.93	3.05	0.15	0.048	0.91
9	block	68.90	0.32	0.005	0.92	3.11	0.15	0.048	0.94
		3rd Post-intervention period ($t_0 + 3$)							
		Linear				Non-Linear			
Pre-int.	Bootstrap	True ATE	Bias	Rel. Bias	Coverage	True ATE	Bias	Rel. Bias	Coverage
4	block	36.67	1.07	0.029	0.92	2.03	0.22	0.110	0.95
9	block	45.93	0.50	0.011	0.94	2.07	0.15	0.074	0.93

Table 9: Simulation results for $N = 200$ units, $\phi = 1.2$ and $\sigma_u = 1$

		1st Post-intervention period ($t_0 + 1$)							
		Linear				Non-Linear			
Pre-int.	Bootstrap	True ATE	Bias	Rel. Bias	Coverage	True ATE	Bias	Rel. Bias	Coverage
4	block	232.58	0.26	0.001	0.94	4.07	0.14	0.033	0.96
9	block	629.30	0.18	0.000	0.94	4.14	0.14	0.033	0.94
		2nd Post-intervention period ($t_0 + 2$)							
		Linear				Non-Linear			
Pre-int.	Bootstrap	True ATE	Bias	Rel. Bias	Coverage	True ATE	Bias	Rel. Bias	Coverage
4	block	174.44	0.62	0.004	0.93	3.05	0.14	0.045	0.93
9	block	471.97	0.37	0.001	0.92	3.11	0.13	0.042	0.93
		3rd Post-intervention period ($t_0 + 3$)							
		Linear				Non-Linear			
Pre-int.	Bootstrap	True ATE	Bias	Rel. Bias	Coverage	True ATE	Bias	Rel. Bias	Coverage
4	block	116.29	1.18	0.010	0.93	2.03	0.14	0.069	0.93
9	block	314.65	0.67	0.002	0.93	2.07	0.13	0.064	0.91

Table 10: Simulation results for $N = 200$ units, $\phi = 1.2$ and $\sigma_u = 0.1$

		1st Post-intervention period ($t_0 + 1$)							
		Linear				Non-Linear			
Pre-int.	Bootstrap	True ATE	Bias	Rel. Bias	Coverage	True ATE	Bias	Rel. Bias	Coverage
4	block	74.24	0.14	0.002	0.94	4.07	0.19	0.046	0.96
9	block	632.26	0.27	0.000	0.94	4.14	0.15	0.037	0.96
		2nd Post-intervention period ($t_0 + 2$)							
		Linear				Non-Linear			
Pre-int.	Bootstrap	True ATE	Bias	Rel. Bias	Coverage	True ATE	Bias	Rel. Bias	Coverage
4	block	55.68	0.22	0.004	0.92	3.050	0.14	0.047	0.91
9	block	474.20	0.55	0.001	0.93	3.100	0.14	0.046	0.95
		3rd Post-intervention period ($t_0 + 3$)							
		Linear				Non-Linear			
Pre-int.	Bootstrap	True ATE	Bias	Rel. Bias	Coverage	True ATE	Bias	Rel. Bias	Coverage
4	block	37.12	0.33	0.009	0.93	2.03	0.22	0.107	0.95
9	block	316.13	1.07	0.003	0.94	2.07	0.15	0.074	0.94

E Additional application material

Table 11: Definition of the variables included in the initial dataset

Dependent variable				
Variable name	Definition	Time period	Source	
Standardized math test score	Standardized math test score of fifth-grade students.	School year 2012/2013-school year 2020/2021	National Institute for the Evaluation of Educational Instruction and Training (INVALSI)	
Time-invariant variables				
Variable name	Definition	Time period	Source	
Economic classification dummies	Without specialization, non-manufacturing (touristic), non-manufacturing (non-touristic), made in Italy, other manufacturing	2011	Italian National Institute of Statistics (Istat)	
Dummy district	LLM with at least one industrial district	2011	Istat	
Regional dummies	A dummy for each of the 20 Italian regions		Istat	
Population dummies	$\leq 10,000$; (10,000; 50,000]; (50,000; 100,000]; (100,000; 500,000]; $>500,000$	2011	Istat	
Share of individuals with a university degree	Share of individuals aged 30-34 with a university degree	2014	Istat	
Share of individuals with a high-school degree	Share of individuals aged 30-34 with a high-school degree	2014	Istat	
Share of urban area	Urban surface / Total surface	2012	Istat	
Share of population in the periphery	Share of population located in municipalities considered as peripheral or ultra-peripheral according to the SNAI classification	2011	Istat	
Number of public libraries	Number of public libraries	2016	Istat	
Number of visitors to museums	Number of visitors to museums, galleries, archaeological sites, and monuments per 100,000 inhabitants	2015	Istat	
Average maximum temperature	30-year average (1980-2010) of maximum air temperature ($^{\circ}\text{C}$)	1980-2010	CAMS European Air Quality Reanalysis Data	
Average minimum temperature	30-year average (1980-2010) of minimum air temperature ($^{\circ}\text{C}$)	1980-2010	CAMS European Air Quality Reanalysis Data	
Average total yearly precipitation	30-year average (1980-2010) of total precipitation (mm)	1980-2010	CAMS European Air Quality Reanalysis Data	
Turnout referendum	Turnout at the constitutional referendum that was held in Italy on 4 December 2016	2016	Ministry of the Interior	
Share of Yes at the referendum	Share of Yes at the constitutional referendum that was held in Italy on 4 December 2016	2016	Ministry of the Interior	
Percentage of children aged 0-2 years who have utilized childcare services	Children aged 0-2 years who have utilized childcare services provided by Municipalities (nurseries, micro-nurseries, or integrated and innovative services) / Resident children aged 0-2 years * 100.	2016	Istat	

Time-varying variables

Variable name	Definition	Time period	Source
Standardized Italian test score	Standardized Italian test score of fifth-grade students.	School year 2012/2013-school year 2018/2019	INVALSI
Percentage of participants to the math test	Percentage of participation in the math test (pupils who took the test out of expected pupils)	School year 2012/2013-school year 2018/2019	INVALSI
Percentage of participants to the Italian test	Percentage of participation in the Italian test (pupils who took the test out of expected pupils)	School year 2012/2013-school year 2018/2019	INVALSI
Average percentage score for math	Average percentage score for math - adjusted for cheating	School year 2012/2013-school year 2018/2019	INVALSI
Average percentage score for Italian	Average percentage score for Italian - adjusted for cheating	School year 2012/2013-school year 2018/2019	INVALSI
Standard deviation for math	Standard deviation of the percentage score for math	School year 2012/2013-school year 2018/2019	INVALSI
Standard deviation for Italian	Standard deviation of the percentage score for Italian	School year 2012/2013-school year 2018/2019	INVALSI
Log of the Gini index	Log of the Gini index	2013-2019	Ministry of Economy and Finance (MEF)
Share of foreign population	Foreigners / population	2013-2019	Istat
Unemployment rate	Resident population aged 15+ not in employment but currently available for work / Labor force	2013-2019	Istat
Share of graduate mayors	Share of municipalities with a mayor with a university degree	2013-2019	Ministry of the Interior
Share of recycled waste	Share of recycled waste	2013-2019	Italian National Institute for Environmental Protection and Research (Ispra)
Share of workers in manufacturing	Share of workers in manufacturing	2013-2019	Istat
Share of old population	Share of population aged ≥ 65	2013-2019	Istat
Declared income per capita	Declared income per capita	2013-2019	MEF
Log of declared income (total)	Log of declared income (total)	2013-2019	MEF
Share of income for pensions	Share of overall declared income for pensions	2013-2019	MEF
Share of income for employment	Share of overall declared income for employment	2013-2019	MEF

Population	Resident population	2013-2019	Istat
Average price per square meter	Average price per square meter - house	2013-2019	Osservatorio del Mercato Immobiliare - Agenzia delle Entrate

Notes. In our application, time-invariant covariates are either features of the LLM not subject to time changes (e.g. area of the LLM) or features taken at a time before 2017. Data from the 2020/2021 school year represent the first available post-pandemic data point for the standardized math test score, as there was no test for the school year 2019/2020 due to the national lockdown. Following [Carlana et al. \(2023\)](#), math test scores have been standardized for the entire dataset using the 2013-2019 values as a benchmark, with a mean of 0 and a standard deviation of 1.

Table 12: Performances with different numbers of variables

Method	MSE		
	10 variables	20 variables	30 variables
LASSO	0.4316	0.4169	0.6559
Partial Least Squares	0.4172	0.4044	0.4156
Boosting	0.3995	0.3909	0.4037
Random Forest	0.4011	0.3902	0.3935

Table 13: Definition of the 20 variables included in the estimation process (random forest)

Predictors	Lag
Standardized math test score	First, second and third
Standardized Italian test score	First, second and third
Average percentage score for math	First, second and third
Change in the average percentage score for Italian	First
Average percentage score for Italian	Second
Change in the average percentage score for Italian	First
Change in the standard deviation for math	First and second
Change in the unemployment rate	Third
Change in the log of declared income (total)	Third
Log of declared income (total)	Third
Share of individuals with a high-school degree	Fixed (2014)
Dummy Calabria	Fixed
Turnout referendum	Fixed (2016)

Notes. These are the 20 variables selected via the panel CV procedure by the preliminary random forest.

Table 14: Definition of the variables included in the data-driven CATEs analysis

Variable name	Definition	Time period	Source
COVID-19 impact on the standardized math test score (dependent variable)	Treatment effect of the COVID-19 crisis on the standardized math test score (SD)	School year 2020/2021	Estimated via the MLCM with random forest
Share of income accruing to low-income earners	Share of income accruing to individuals with an overall income $\leq 26,000$ Euro	2019	MEF
Average download speed of the internet	Average download speed of the internet	2018	AGCOM
Share of households without internet access	Share of households without internet access	2018	AGCOM
Tourism LLM	Dummy variable equal to 1 for LLMs specialized in tourism	2011	Istat
Share of individuals with a university degree	Share of individuals aged 30-34 with a university degree	2015	Istat
Population	Resident population	2019	Istat
Per capita expenditure on gambling	Per capita expenditure on gambling	2019	
Unemployment rate	Resident population aged 15+ not in employment but currently available for work	2019	Istat
Excess mortality estimates	Municipality-level excess mortality estimated by applying ML techniques to all-cause deaths data, aggregated at the LLM level	From Feb 21, 2020 to Sep 30, 2020	(Cerqua et al., 2021)
Share of temporary contracts	Number of employees with temporary contracts in October divided by the number of employees in October	2015	Istat
Share of jobs in suspended economic activities	Share of jobs in activities suspended in March 2020 by the Italian Government due to the spread of the pandemic	2017	Istat
Per capita income	The amount of money earned per person	2019	MEF
Share of firms having employees in short-time work subsidies	The number of firms with employees receiving short-time work subsidies divided by the universe of firms registered in the Business Register	Average (2015-2018)	Ministry of Labor and Social Policies
Share of population living in peripheral areas	Share of population living in areas defined by Istat as peripheral or ultra-peripheral	Jan 1, 2020	Istat
Dependency ratio	The ratio of those typically not in the labor force (the dependent part, ages 0 to 14 and 65+) and those typically in the labor force (the productive part, ages 15 to 64)	Jan 1, 2020	Istat
Gini index	Gini index	2019	MEF
Average price per square meter	Average price per square meter - house	2019	Osservatorio del Mercato Immobiliare - Agenzia delle Entrate

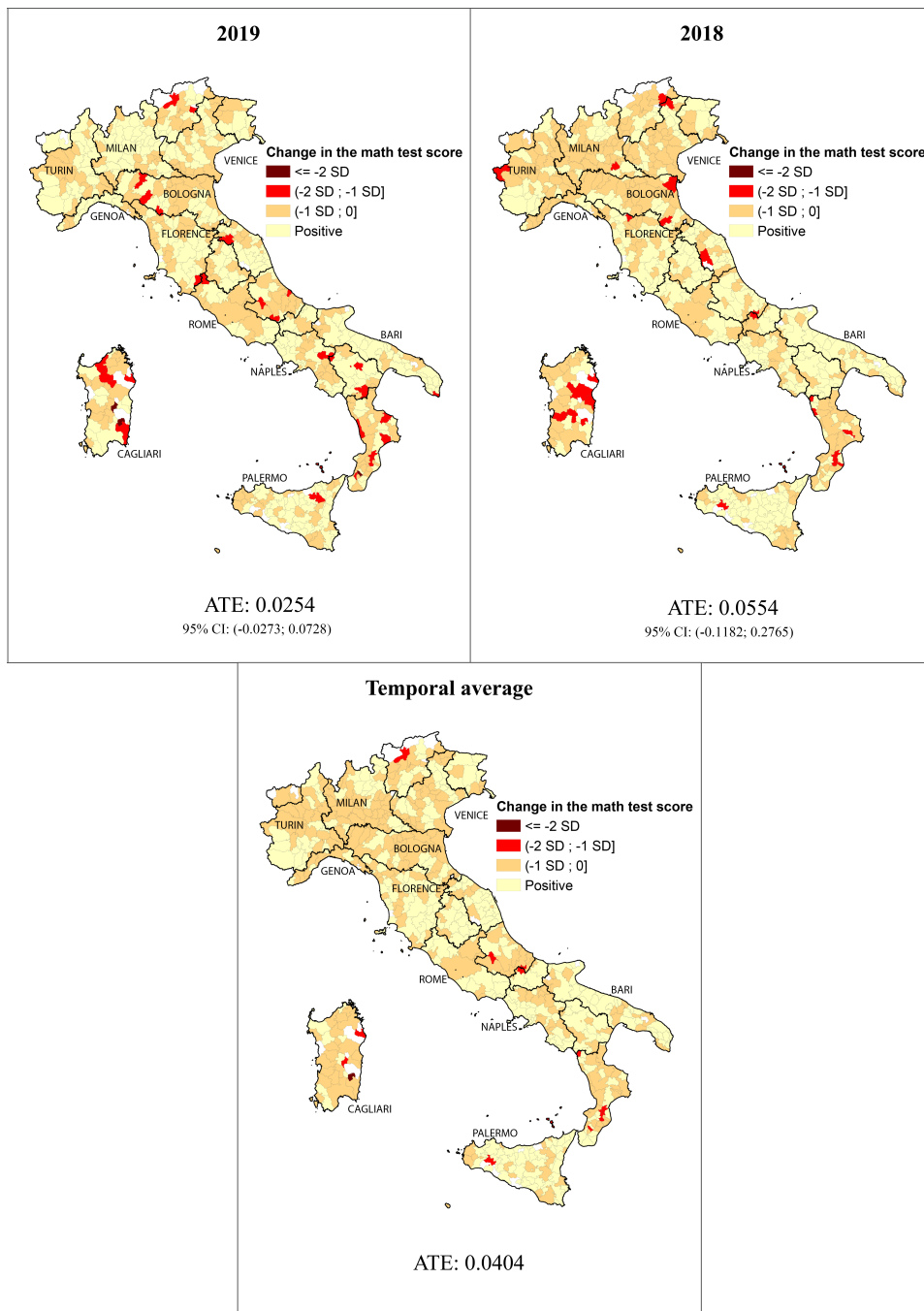


Figure 6: Unit-level panel placebo test by year

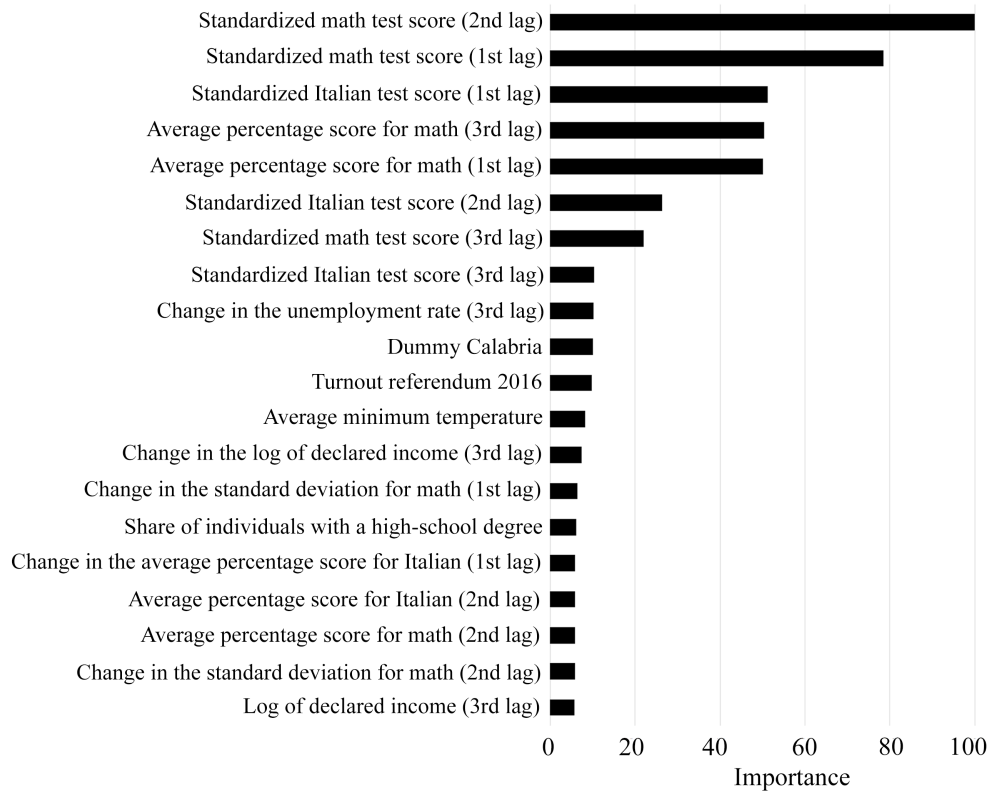


Figure 7: Variable importance ranking – Preliminary random forest